UNIVERSITY OF NAIROBI

COLLEGE OF ARCHITECTURE AND ENGINEERING

SCHOOL OF ENGINEERING

DEPARTMENT OF MECHANICAL AND MANUFACTURING ENGINEERING

PROJECT TITLE

PERFORMANCE EVALUATION OF AN EXISTING SOLAR CONCENTRATOR

A final year project report submitted in partial fulfillment of the award of the Bachelors degree in Mechanical Engineering of the University of Nairobi.

AUTHORS:

SUGE MARTIN SOY F18/2421/2009

MOKAYA ABEL MENGE F18/2449/2009

SUPERVISOR: DR.A.A.AGANDA

DECLARATION

We declare that this is our original work and has not been presented for a degree in any other University or institution of learning.

SUGE MARTIN SOY F18/2421/2009: **Date:**

_____ _____

MOKAYA ABEL MENGE F18/2449/2009: **Date:**

_____ _____

This project is submitted as part of the examination board requirements for the award of the **Bachelor of Science** degree **in Mechanical and Manufacturing Engineering** from **the University of Nairobi**

PROJECT SUPERVISOR: DR.A.A AGANDA **Date:**

_____ _____

DEDICATION

This project is dedicated to our parents for their undying efforts to educate us this far, the Mechanical Engineering Department of the University of Nairobi and to the society in general.

ACKNOWLEDGEMENTS

We would like to express our gratitude and appreciation to all those who made it possible for us to complete this report. A special thanks to our final year project supervisor, Dr. A. A. Aganda, whose help, stimulating suggestions and encouragement, helped coordinate our project especially in writing this report.

We would also like to acknowledge with much appreciation Mr. Wilson Kariuki who designed and fabricated the Parabolic Trough Concentrator (PTC) as part of his Master's Thesis. He was also of great help in giving us an orientation of the general experimental procedures.

We would like to acknowledge with much appreciation the crucial role of the staff of Mechanical Engineering Workshop, whose technical assistance and provision of necessary material enabled us complete the fabrication of the orifice meter. Special thanks to Mr. John Kahiro, Mr. Peter Kogi, Mr. Kenneth Karanja, Mr. James Kimani, Mr. Simon Maina and Mr. Jackton Anyona.

Lastly, we wish to thank the Department of Mechanical and Manufacturing Engineering for the support and funding of this project to make it a success.

ABSTRACT

The main sources of energy in the world are based on fossil fuels. However, these sources have several downsides such as causing damage to the environment and they are also sensitive to price changes. Due to the above shortcomings, solar energy is increasingly being utilized in different parts of the globe. One of the solar technologies being used is the parabolic trough concentrator (PTC). It produces high temperatures that may not be attained by open sun drying or flat plate collectors. High temperatures are appropriate for high rates of drying and in situations where the only limitation is the prevention of self-ignition. Typical cases are in drying of biomass.

An orifice meter was fabricated at the Mechanical Engineering Workshop, University of Nairobi. It was used to measure the mass flow rate of air through the receiver tube of a PTC.

A PTC designed and fabricated by Mr. Wilson Kariuki was used for the experimentation [**16**]. The experiments were carried out between 1000hrs and 1600hrs on selected days between 26rdFebruary and 02ndApril 2014. Throughout the experimentation, the PTC was covered with glass and a 50.8mm diameter receiver tube used. Mass flow rates of 0.001493kg/s, 0.002986kg/s, 0.004472kg/s, 0.00538kg/s, 0.006678kg/s, 0.007483kg/s, 0.008846kg/s were used.

The highest temperature was recorded while using a mass flow rate of 0.001493kg/s and it was 105.6°C while that recorded while using a mass flow rate of 0.008846kg/s was 72.9°C. It was therefore evident that higher outlet temperatures were obtained at low mass flow rates.

The maximum useful energy obtained from the PTC with a mass flow rate of 0.001493kg/s was 101.86J/s while that obtained with a mass flow rate of 0.008846kg/s was 395.05J/s. This indicated that useful energy is directly proportional to mass flow rate.

Overall efficiencies calculated while using mass flow rates of 0.001493kg/s and 0.008846kg/s were 3.5% and 10.74% respectively. This implied that overall efficiency increases with increase in mass flow rate.

Table of Contents

LIST OF SYMBOLS

A_{ap} Aperture area (m^2)

A_i Inner tube area (m^2)

A_o Outer tube area (m^2)

C_p Specific heat capacity at constant pressure.

d Orifice size

D Diameter of tube (m)

D_o Outer tube diameter (m)

F' Collector efficiency factor

F_R Heat removal factor

Gr Grashof number

h Heat transfer coefficient ($W/m^2°C$)

h_f Heat transfer coefficient inside the absorber tube ($W/m^2°C$)

I Total radiation (W/m^2)

k Thermal conductivity

$\dot{m}$ Mass flow rate

Nu Nusselt number

Pr Prandtl number

Ra Rayleigh number

Re Reynolds number

T_a Ambient temperature

T_i Inlet fluid temperature

$T_{m,f}$ Mean film temperature

T_o Outlet fluid temperature

U_l Overall heat loss coefficient ($W/m^2°C$)

W Aperture width

α Absorptivity of receiver pipe

β Thermal expansion factor

β_1 Ratio of orifice diameter to receiver tube diameter

ε Emissivity

η Efficiency

ρ Reflectance of the reflective surface

σ Stefan Boltzmann's constant (=5.67×10^{-8} W/m^2K^4)

τ Transmittance

υ Kinematic viscosity (m^2/s)

θ_r Rim angle

ABBREVIATIONS

PTC Parabolic trough concentrator

w.b. Wet basis

CHAPTER 1

INTRODUCTION

1.1 Background

The main sources of energy in the world are; oil (38%), coal (26%), gas (23%), hydroelectric (6%) and nuclear (6%). Geothermal, solar, wind and wood only contribute a paltry 1%. As the world continues to develop, the demand for energy will continue to rise.

The three main sources of energy are based on fossil fuels and they have many downsides. First and foremost, they cause damage to the environment by depleting the O-zone layer. While being heated to produce energy, they give out green house gases such as CO_2 that contribute immensely to global warming and climatic changes [**1**]. These three main sources are also sensitive to price changes and may lead to global conflicts in the future. There is therefore need for the world to advance towards renewable energy in order to mitigate these disadvantages. Governments give incentives via policies to encourage investments in renewable energy.

The annual solar radiation reaching the earth's surface, approximately 3 400 000 EJ, is an order of magnitude greater than all the estimated (discovered and undiscovered) non-renewable energy resources, including fossil fuels and nuclear. If only a fraction of this could be utilized then this would go a long way to satisfy the world's energy demand.

Solar energy doesn't make any contribution to Kenya's national grid. The total grid installed capacity was 1712MW as of June 2012[**2**] . It consisted of 812MW-hydro, 646MW-thermal, 205.8MW-geothermal, 5.1 MW wind, 26MW-cogeneration, 18MW-isolated grid. The isolated grid power was obtained from burning of fossil fuels.

Open sun drying of food has been practiced since the ancient times. Its main advantages include; low capital and initial costs and no expertise is required. However it has several limitations such as; contamination, theft or damage by birds, no protection from rain or dew, large areas of land needed, direct exposure to the sun also reduces quality (color and vitamin content) [**3**].

The above disadvantages are significantly reduced by the use of solar dryers. Solar dryers are being used all over the world to dry agricultural products. They enable the user to control the drying conditions such as the drying temperature [**3**]. This enhances the production of good quality agricultural products. They also reduce the drying time required. For example, the Hohenheim tunnel dryer has been used to dry fish in Bangladesh. Here, 150 kg of Silver Jew fish were dried from 66% w.b. to 16% w.b. in five days. Comparable samples dried with the traditional methods had a moisture content of 32.84% w.b. after five days. It has therefore reduced the drying time of fish by 50% [**4**]. A solar maize dryer incorporating a directly coupled photo voltaic (PV) powered D.C fan was developed and field-tested for small scale use in Malawi. Drying using this technology reduced the drying time by over 70%. Grain texture, flour quality and flavor improved significantly with the dryer, as grain was protected from sudden rains, vermin and dust contamination.

The main application of PTCs is in power generation. They are being used to heat thermal fluids such as oil and molten salts that are eventually used to generate steam for turning turbines.
The PTC consists of a parabolic trough of large area that concentrates the sun's radiation onto a receiver pipe of a much smaller area. This results in a very high intensity radiation on the pipe. The PTC is therefore able to heat air to higher temperatures than flat plate collectors. However PTCs are currently not being used to dry biomass even though they are suitable to do so. A PTC built with locally available inexpensive materials can heat air to between 100-130°C, suitable for drying biomass.

Biomass such as bagasse and municipal waste can be dried and used as boiler fuels. In Kenya, bagasse is being used by Mumias Sugar Company to generate electricity while municipal waste is not being used at all. Mumias Sugar feeds the bagasse directly to the boilers without drying. This results in wastage of energy since some of the heat is used to vaporize water present in the bagasse. Drying will therefore result in increased boiler efficiency.

1.2 Problem statement

In Kenya, power generation using fossil fuels accounts for 38% of the installed capacity [**2]**. Fossil fuels have several disadvantages that include; emission of green house gases that cause global warming, they are subject to constant price increase, drying up of terrestrial fossil fuels. It is the above shortcomings that have led to the shift towards renewable sources of energy. Solar energy is free, environmentally clean and sustainable. Kenya has a great potential for solar energy utilization throughout the year due to its strategic location near the equator.

Biomass such as municipal waste and bagasse can be used to generate electricity. Bagasse is currently being used by Mumias Sugar Company to generate 36MW of power through cogeneration. It sells 26MW to the National Grid while it consumes the rest. Here, bagasse is fed into boilers at a moisture content of around 50%. This significantly limits the efficiency of the boiler since part of the heat is wasted in evaporating the moisture present in the bagasse. There is therefore need for research into cheap methods of drying the bagasse. One potentially good method is the use of the PTC.

Very few experiments have been carried out on PTCs in Kenya hence little information exists on the same. It is therefore relevant to carry out extensive experiments in order to determine the performance of a PTC under different operating and weather conditions.

1.3 Objectives

The overall objective of this study is to test the performance of an existing PTC. The specific objectives are:

1. Design and fabricate an orifice meter to be incorporated into the PTC.
2. Evaluate the performance of the PTC using different mass flow rates.

CHAPTER 2

LITERATURE REVIEW

2.0 Introduction

This chapter gives a brief review of the various methods of solar drying being employed in different parts of the world. It also describes selected methods of biomass drying.

2.1 Solar Drying

The main objective of drying an agricultural product is to reduce its moisture content sufficiently in order to prevent deterioration within the period of storage. Drying is a dual process of heat and mass transfer. Heat transfer takes place between the source of heat and the product whereas mass transfer of moisture takes place between the interior of the product to its surface; then from the surface to the surrounding air.

In solar drying, solar energy is used as either the sole or a supplemental source of heat; air flow can be generated by either forced or natural convection. The heating procedure could involve the passage of preheated air through the product, by directly exposing the product to solar radiation or a combination of both. The major requirement is the transfer of heat to the moist product by convection and conduction from surrounding air mass at temperatures above that of the product, or by radiation mainly from the sun and to a little extent from surrounding hot surfaces, or conduction from heated surfaces in contact with the product. Water starts to vaporize from the surface of the moist product when the absorbed energy has increased its temperature sufficiently from the water vapor pressure of the crop moisture to exceed the vapor pressure of the surrounding air.

There are two main types of solar drying i.e. open sun drying and sun drying using driers. These drying methods are reviewed in the following section.

2.1.1 Open Sun Drying (OSD)

Open sun drying has been used since time immemorial to dry different materials including agricultural products. It involves spreading the product on the ground and utilizing the sun's direct radiation and natural air movement to dry the product.

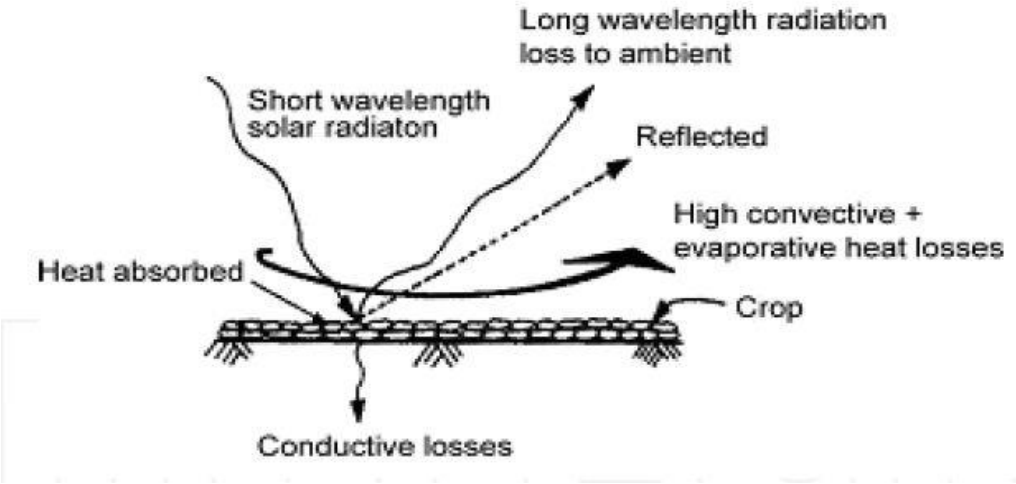

Figure 2.1: Open sun drying [3]

Short wavelength solar radiation falls on the uneven product surface. Part of the energy is reflected back to the atmosphere while the rest is absorbed by the product. The rate of absorption is directly proportional to the color of the product. Dull colored products will absorb more energy than the bright colored products. The absorbed energy is then converted into thermal energy and the temperature of the product starts to rise. The product then emits long wavelength radiation to the ambient air via moist air. There is also convective heat loss due to wind blowing over the product being dried. Evaporation of moisture also results in evaporation losses.

A part of the absorbed energy is absorbed into the interior of the product. This results in a temperature rise and formation of water vapour in the material. The water vapour then diffuses towards the surface of the product and finally energy is lost in the form of evaporation.

Initially the moisture removal is rapid since excess moisture on the surface of the product presents a wet surface to the drying air. Subsequently, drying depends on the rate at which the moisture within the product moves to the surface by the diffusion process. This in turn depends on the type of product being dried.

The advantages of open sun drying are low capital investment, low operating costs and little expertise is required. However, OSD has numerous disadvantages which make it unsuitable for drying materials. They include; biological losses due to rodents, birds insects and micro-organisms, unexpected rain can cause damage to the product, contamination by foreign materials, discoloring by U.V radiation. In general, OSD does not fulfill the international quality standards of drying food. Due to the above mentioned shortcomings, use of solar driers has been employed.

2.2 SOLAR DRIERS

2.2.1 Passive solar dryer

Here, air is heated then circulated naturally by buoyancy force or as result of wind pressure or a combination of both. There are three main types; direct, indirect or mixed. Heated air has lower density than cool air at the same pressure. This results in vertical air flow. They are cheap and simple to build. However, the rate of drying in these driers is lower than in active solar driers [**3**].

2.2.1.1 Direct type Solar Dryer (DSD)

Direct type solar drying is also known as natural convection solar drying. This type of solar drying utilizes the natural movement of air in drying the product. Part of the incident ray that lands on the transparent cover is reflected back to the atmosphere while the rest is transmitted through the cover. Furthermore, part of the transmitted radiation is reflected back from the surface of the product while the rest is absorbed by the product. The radiation absorbed causes the temperature of the product to increase. The product then starts emitting long wavelength radiation which is not allowed to escape to the atmosphere due to the presence of a glass cover. This therefore causes the temperature inside the chamber to gradually rise. The glass cover also reduces losses via direct convection to the atmosphere which results in a further rise of the chamber temperature (Sharma et al., 2009).

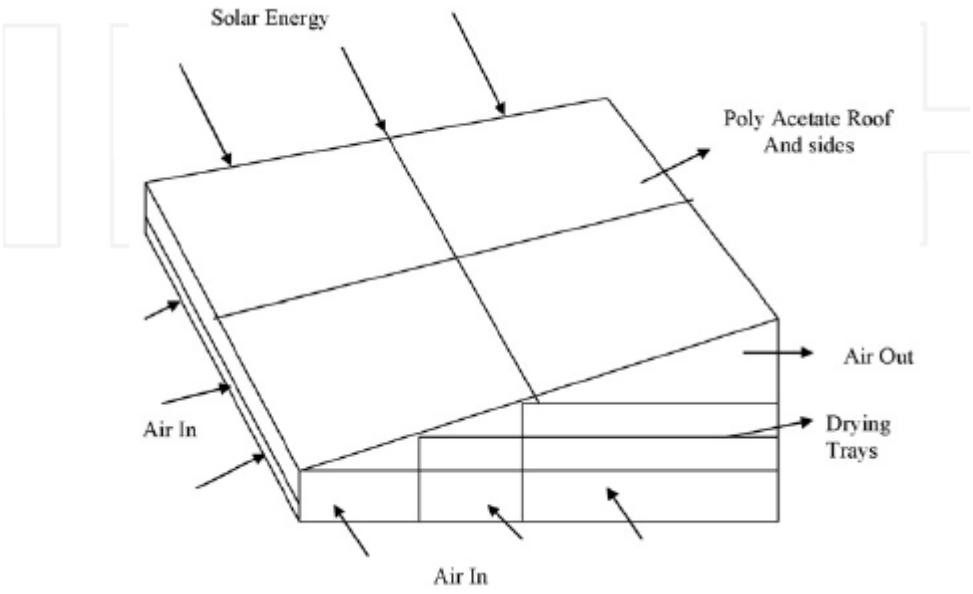

Figure 2.2: Direct solar drier [3]

The dryer consists of a drying chamber covered by a transparent material. This material can be either glass or plastic. The chamber is usually a shallow, insulated box with air holes in it to allow air to enter and exit freely. The product is placed on a perforated tray that allows air to pass through it and the material being dried. (Refer to **fig. 2.2**).

This type of dryer can achieve temperatures of between 50°C to 100°C.

Ekechukwu and Norton (1999) reported a modification of the typical design. The cabinet dyer was equipped with a wooden plenum to guide the air inlet and a long plywood chimney to enhance natural circulation. This dryer was reported to have accelerated the drying rate about five times open sun drying [**3**].

2.2.1.2 Indirect type Solar Dryer (ISD)

As the name suggests, the product being dried is not directly exposed to the sun's radiation. This ensures that discoloration and cracking on the surface of the product is minimized. It is useful in drying products such as tomatoes which is discolored by direct radiation.

A separate unit termed the solar air heater is used to heat the air. It consists of a flat plate collector enclosed in a chamber which is covered with a transparent glass. The air is then directed to an opaque drying chamber which houses the product.

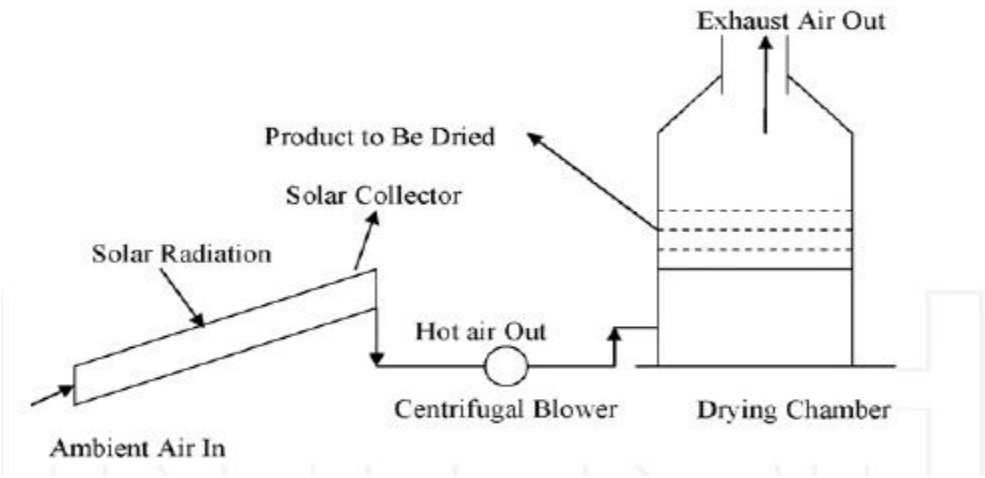

Figure 2.3: Indirect solar drier [4]

The heated air is allowed to flow through the wet material. Here, the heat for moisture evaporation is provided by convective heat transfer between the drying air and the air in the vicinity of the product surface.

This type of dryer gives a better control over drying and the product obtained is of good quality.

There are several types of solar dryers that have been developed to serve various purposes. The popular ones are natural convection cabinet type, green house type and the solar tunnel drier.

2.2.1.3 Mixed Mode Solar Driers (MSD)

This type of solar dryer employs features from both the direct solar dryer and the indirect solar dryer. The heat used for drying is obtained by both direct solar radiation and from air preheated in a solar air chamber. The temperature obtained in the drying chamber is higher than in both the direct and indirect types of solar driers.

2.2.1.4 Hybrid Solar Driers

Hybrid solar driers combine solar energy with a fossil fuel such as rice husks. This type of dryer helps ensures that drying continues uninterruptedly even in the case of poor weather or during night times. They therefore solve some of the disadvantages of direct, indirect and mixed mode dryers. It is interesting to note that 100kg of rice yields 200kg of rice husks. It only requires 20kg of rice husks to be dried (Hislop, 1992

2.2.2 Active Solar Driers

These driers are designed to incorporate an external means of pushing air into the drying chamber. They usually employ the use of fans to cause air to flow by forced convection inside the drying chamber. Optimum air flow can be provided in the drier throughout the drying process to enable control of temperature and moisture independent of the weather conditions. The use of forced convection can reduce the drying time by up to three times and reduce the collector area by 50% [**3**].

Just like passive solar driers, there are three types of active solar driers; direct, indirect, mixed mode and hybrid. There design is similar to the passive types except that they have a fan at the air inlet part. They also don't have a chimney.

2.3 APPLICATIONS OF SOLAR DRYERS

2.3.1 Fish Drying

Fish contains up to 80% of water and it is a highly perishable material. When moisture content is reduced to 25% w.b., contaminating agents cannot survive and autolytic activity is greatly reduced. However, fish is dried to 15% moisture content to prevent mould growth during storage. Tropical species of fish can withstand temperatures of 45°C to 50°C before proteins are denatured and cooking starts [**4**].

The Hohenheim tunnel dryer has been used to dry fish in Bangladesh. Here, 150 kg of Silver Jew fish were dried from 66% w.b. to 16% w.b. in five days. Comparable samples dried with the traditional methods had a moisture content of 32.84% w.b. after five days. The temperature of the drying air at the collector outlet varied from 35.1°C to 52.2°C during drying. The fish was initially treated with dry salt and stacked for about for about 16 hours before commencement of drying.

2.3.2 Drying of Maize Grains

A solar maize dryer incorporating a directly coupled photo voltaic (PV) powered D.C fan was developed and field-tested for small scale use in Malawi. The dryer has a capacity of 90kg and it has been designed to utilize forced air circulation without the use of any external power supply like grid electricity, fossil fuels and batteries. A main design constraint was the fact that the drying temperature should not exceed 60°C, which is international drying standard of maize grains to be used for human consumption.

Temperatures in excess of 60°C lead to grain overheating, cracking and microbial attack. Results revealed that the incorporation of a P.V driven fan provided some form of passive control over the air flow and hence the drying air temperature.

The dryer was coupled to a solar air heater having a sun-tracking facility and optimized blackened sisal rope grids for improved energy collection efficiency of the order of 80%.

Grain drying with this solar drying technology reduced the drying time by over 70%. Grain quality texture and flour quality and flavor improved significantly with the dryer, as grain was protected from sudden rains, vermin and dust contamination. Although the capital cost was about $900, the dryer was found to be cost effective with a payback period of less than one year if it is used to dry grain for purchase by Cereals Board.

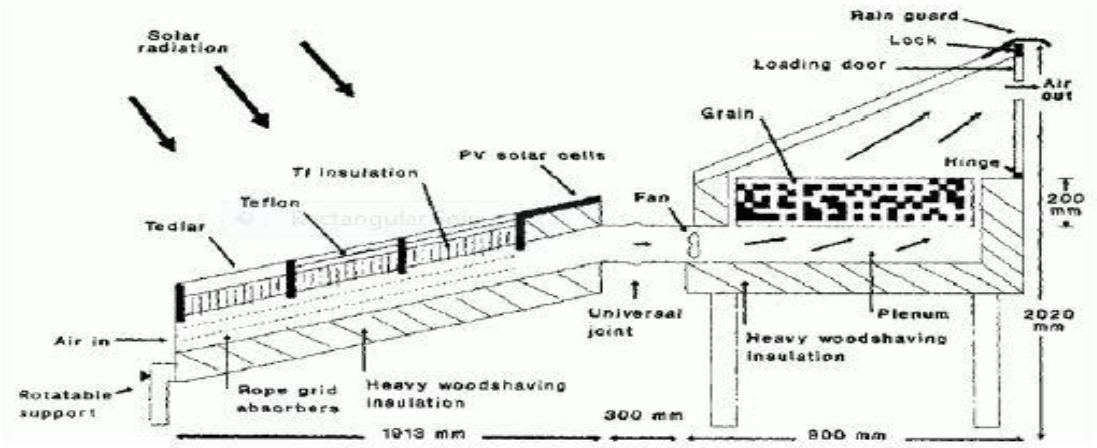

Figure 2.4: Solar grain dryer with rotating indirect air heater and a photo voltaic D.C fan [4]

2.3.3 Medium Scale Coffee Drying in Kenya

Action is currently being taken in Kenya to improve the drying techniques for parchment coffee in smallholder co-operative factories. The Thailand Development Research Institute is responsible for the design, installation and commissioning of three drying installations based on a solar assisted drying process. The construction of the first of these was completed and commissioned at Rukera in November 1983. The drying bins are contained in a building of which the roof forms a simple bare plate solar collector black painted corrugated iron with a hardboard ceiling suspended 30 cm beneath it. Air is drawn through the cavity between the roof and ceiling by means of a diesel-powered fan, the air being drawn also around the diesel engine block before entering the fan and being propelled into the drying bins. Temperature increases of up to 15 °C have been obtained by passage of air at 8.5 m^3/s across the roof cavity, with an additional 3-4 °C increase derived from the waste heat of the engine.

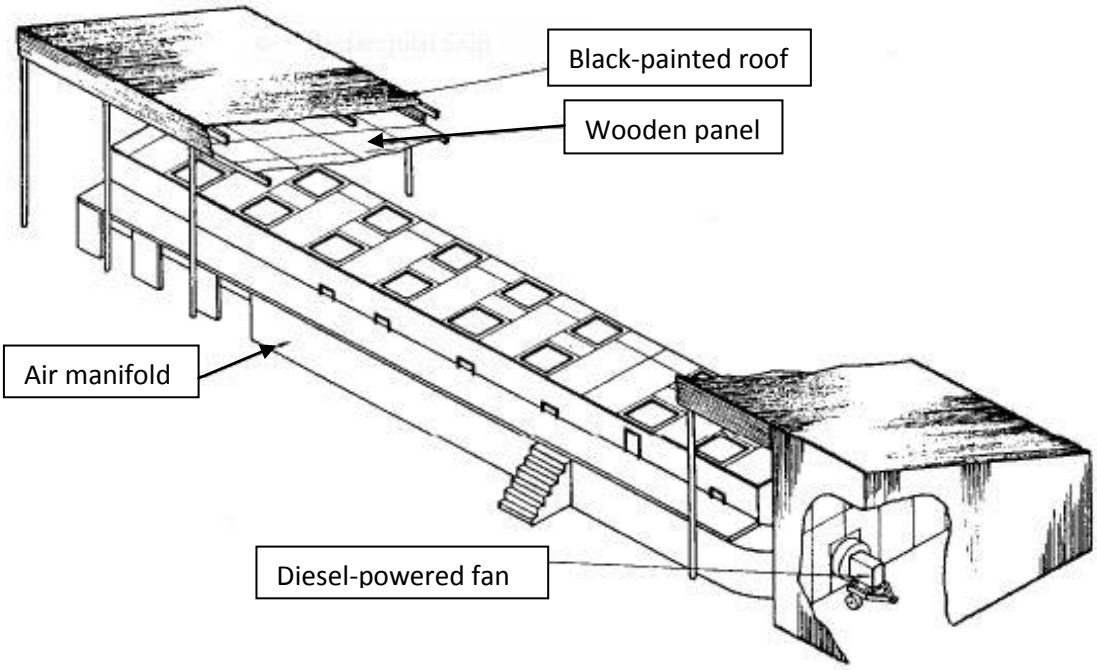

Figure 2.5: Thailand Development Research Institute parchment coffee drying system [4].

2.3.4 Banana Dryer, Brazil

The solar dryer system introduced by Costa is operating in a mixed mode. It uses indirect heating through forced convection, which gives high yield and good quality for the dried product.

The system is composed of:

- An electrical ventilator allowing an independent air flow rate;
- A solar collector in which its characteristics and dimensions were determined according to hot air flow rate and operating temperature;
- A special designed dryer for tropical fruits.

A scheme of the solar dryer is shown below. The innovation of this work is not only in the dryer design and dimension, but also in its configuration, material and in the solar collector dimension. The collector was constructed in such a way that its use can be versatile. It is made of flexible PVC, in a cylinder shape with two cones at the both ends. At the bottom, 50% of the collector is made of dark plastic in order to absorb heat and at the top with transparent plastic, in which the solar rays penetrate.

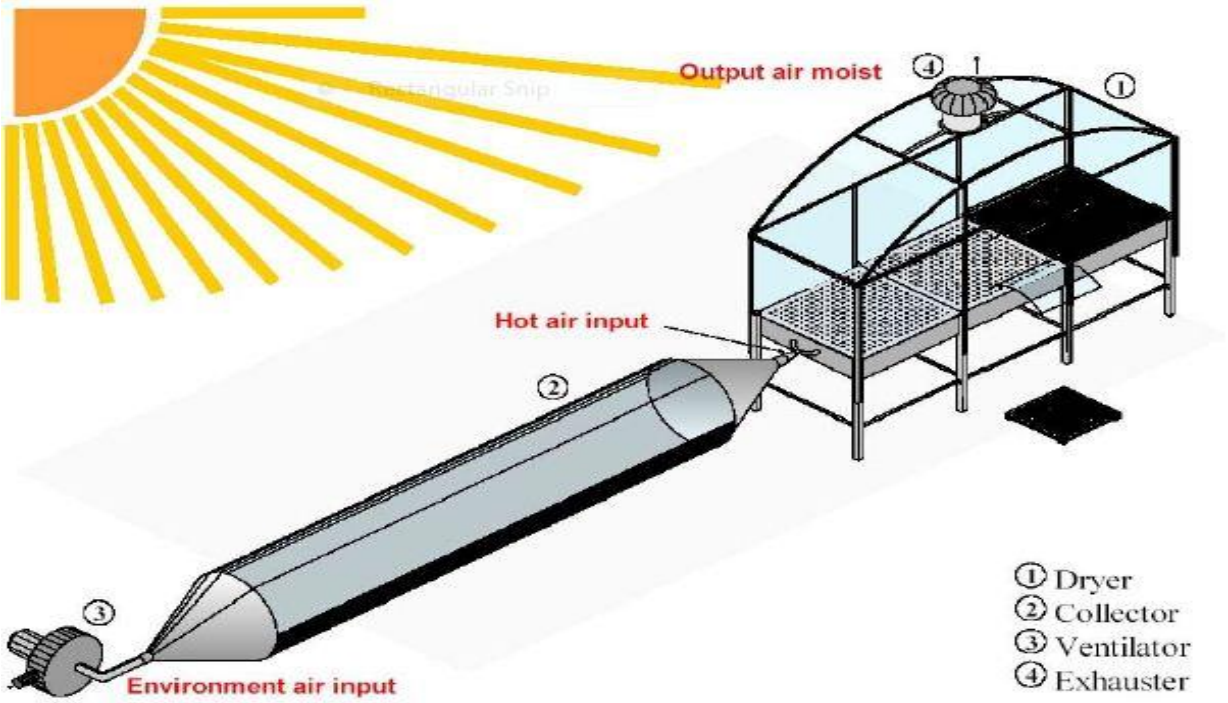

Figure 2.6: Scheme of the solar banana dryer [4].

The dryer also works as a solar collector, because it was constructed of transparent PVC and the aluminium support offers good heating and transport conditions. The trays, which contain the fruits to be dried, can be arranged one on top of the other. An exhauster provides air circulation, through an exit in the superior part.

2.4 SOLAR COLLECTORS

Concentrating, or focusing collectors intercept direct radiation over a large area and focus it onto a small absorber area.

These collectors can provide high temperatures more efficiently than flat-plate collectors, since the absorption surface area is much smaller. However, diffused sky radiation cannot be focused onto the absorber.

Most concentrating collectors require mechanical equipment that constantly orients the collectors toward the sun and keeps the absorber at the point of focus.

Therefore; there are many types of concentrating collectors

2.4.1 Parabolic dish system

A parabolic dish collector is similar in appearance to a large satellite dish, but has mirror-like reflectors and an absorber at the focal point. It uses a dual axis sun tracker.(see fig 2.7)

A parabolic dish system uses a computer to track the sun and concentrate the sun's rays onto a receiver located at the focal point in front of the dish. In some systems, a heat engine, such as a Stirling engine, is linked to the receiver to generate electricity. Parabolic dish systems can reach 1000 °C at the receiver, and achieve the highest efficiencies for converting solar energy to electricity in the small-power capacity range.

Engines currently under consideration include Stirling and Brayton cycle engines. Several prototype dish/engine systems, ranging in size from 7 to 25 kW have been deployed in various locations in the USA. High optical efficiency and low start up losses make dish/engine systems the most efficient of all solar technologies. A Stirling engine/parabolic dish system holds the world's record for converting sunlight into electricity. In 1984, a 29% net efficiency was measured at Rancho Mirage, California.

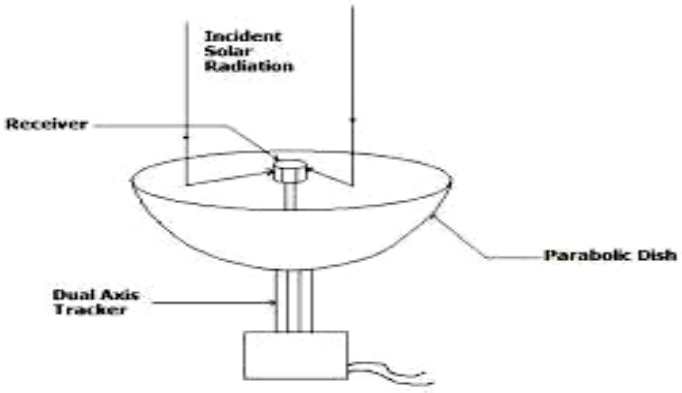

Figure 2.7:parabolic dish system

2.4.2 Power tower system

A heliostat uses a field of dual axis sun trackers that direct solar energy to a large absorber located on a tower (see fig 2.8). To date the only application for the heliostat collector is power generation in a system called the power tower.

A power tower has a field of large mirrors that follow the sun's path across the sky. The mirrors concentrate sunlight onto a receiver on top of a high tower. A computer keeps the mirrors aligned so

the reflected rays of the sun are always aimed at the receiver, where temperatures well above 1000°C can be reached. High-pressure steam is generated to produce electricity.

Heliostat field collector can be suitable for drying of biomass. However, a heat exchanger must be installed so as to transfer heat from steam generated to air. Its construction is relatively more complex and costly.

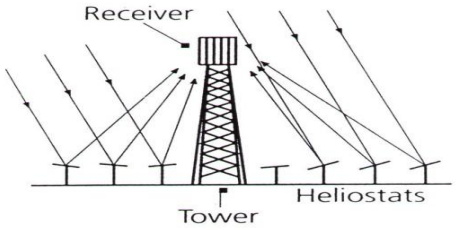

Figure 2.8: Heliostat

2.4.3 Stationary concentrating solar collectors

These are non-imaging concentrators. Stationary concentrating collectors use compound parabolic reflectors and flat reflectors for directing solar energy to an accompanying absorber or aperture through a wide acceptance angle. Acceptance angle being double the angle between the axis of the CPC and the line connecting the focus of one of the parabola with the opposite edge of the aperture.

The wide acceptance angle for these reflectors eliminates the need for a sun tracker.

The main advantage of using a CPC is that it could offer a higher geometrical concentration gain with a narrow field of view [5]. This class of collectors includes parabolic trough flat plate collectors and flat plate collectors with parabolic boosting reflectors, whose developments have been done in Sweden.
Since temperatures achieved are low (between 45^0 and 70^0) , the collector is not suitable for drying of biomass.

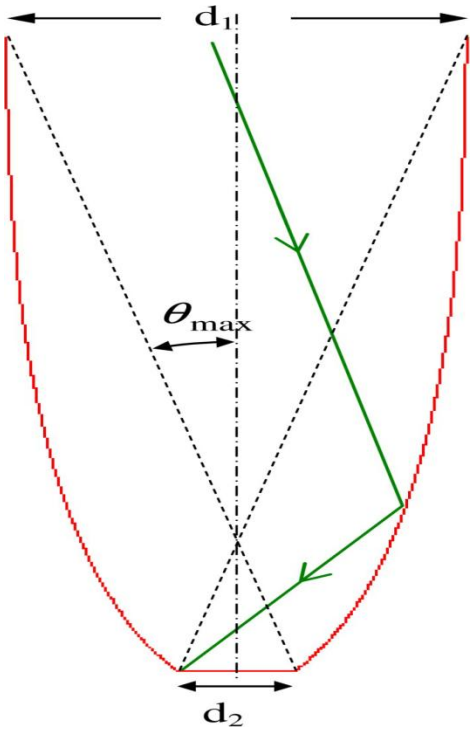

Figure 2.9: Compound parabolic collector

2.4.4 Linear Fresnel reflectors

A linear Fresnel reflector power plant uses a series of long, narrow, shallow-curvature mirrors to focus light onto one or more linear receivers positioned above the mirrors. On top of the receiver a small parabolic mirror can be attached for further focusing the light. The system can be imagined as broken-up parabolic trough collector, but unlike the parabolic troughs, it doesn't have to be parabolic in shape.

These systems aim to offer lower overall costs by sharing a receiver between several mirrors (as compared with trough and dish concepts), while still using the simple line-focus geometry with one axis for tracking. This is similar to the trough design (and different from central towers and dishes with dual-axis). The receiver is stationary and so fluid couplings are not required (as in troughs and dishes). The mirrors also do not need to support the receiver, so they are structurally simpler. When suitable aiming strategies are used (mirrors aimed at different receivers at different times of day), this can allow a denser packing of mirrors on available land area.

An example is the Puerto Errado 1 plant built by the German group Novatec Biosol in March 2009 [**6**].It occupies an area of approximately 18000 m^2, capacity of 1.4MW and an expected production of

2000MWh annually. The steam is generated by concentrating sunlight directly on a linear receiver which is 800m long and 7.4m above the ground. An absorber tube is positioned in the focal line of the mirror field where water is heated to 270^0C.

With the incorporation of a heat exchanger, a linear Fresnel reflector field can be useful in drying biomass.

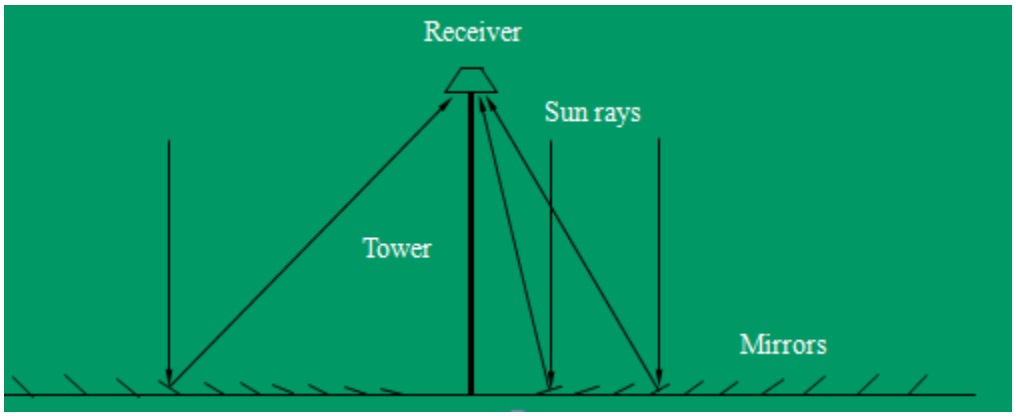

Figure 2.10: Linear fresnel reflector

2.4.5 Parabolic trough

These solar collectors use mirrored parabolic troughs to focus the sun's energy to a fluid-carrying receiver tube located at the focal point of a parabolically curved trough reflector.

The trough is parabolic along one axis and linear in the orthogonal axis. For change of the daily position of the sun perpendicular to the receiver, the trough tilts east to west so that the direct radiation remains focused on the receiver. However, seasonal changes in the in angle of sunlight parallel to the trough does not require adjustment of the mirrors, since the light is simply concentrated elsewhere on the receiver. Thus the trough design does not require tracking on a second axis tracking mechanism is however necessary to enable parabolic trough collector to follow the sun with a certain degree of accuracy. It must also track during periods of irregular cloud cover.

Sometimes a transparent glass tube envelops the receiver tube to reduce convective heat loss.

When the parabola is pointed towards the sun, parallel rays incident on the reflector are concentrated onto the receiver tube

Temperatures at the receiver can reach 400 °C and produce steam for generating electricity. In California, multi-megawatt power plants were built using parabolic troughs. The illustration is as shown in fig 2.11.

Figure 2.11: Parabolic troughs used for power generation [5]

Mirror precision is important and conventional methods to fabricate precision parabolic mirrors are complex and costly. The reflectivity of the surface materials is an important factor in the optical efficiency. In solar energy applications, back silvered glass plates, anodized aluminum sheets and aluminized plastic films serve as reflectors. They are widely commercially available. Films are usually adhered to a supporting material such as aluminium. However, the supporting material must be held with a precision parabolic shape by some supporting structures.

The Luz system collectors adopted by the National Renewable Energy Laboratory (NREL) represent the standard by which all other collectors are compared

The receiver is a 4-meter-long, 70-mm diameter stainless steel tube with a special solar-selective absorber surface, surrounded by an anti-reflective evacuated 115-mm diameter glass tube. Located at the mirror focal line of the parabola, the receiver heats a special heat transfer fluid as it circulates through the receiver tube.

The receiver has glass-to-metal seals and metal bellows to accommodate for differing thermal expansions between the steel tubing and the glass envelop. They also help achieve the necessary vacuum-tight enclosure.

The vacuum-tight enclosure primarily serves to significantly reduce heat losses at high-operating temperatures. It also protects the solar-selective absorber surface from oxidation.

The selective coating on the steel tube has good solar absorptance and a low thermal emittance for reducing thermal radiation losses. The glass cylinder features an anti-reflective coating to maximize the solar transmittance. Getters—metallic compounds designed to absorb gas molecules—are installed in the vacuum space to absorb hydrogen and other gases that permeate into the vacuum annulus over time.

The original Luz receiver design suffered from poor reliability of the glass-to-metal seal. Solel Solar Systems and Schott Glass have developed newer designs that have substantially improved.

The nine separate trough power plants called Solar Energy Generating Systems (SEGS) built in the 1980s in the Mojave Desert, Southeastern California by the Israeli company Bright Source Energy have a combined capacity of 354MW. The collectors used have an aperture width, focal length, length per collector, receiver diameters and peak optical efficiency in the ranges 2.55-5.76m, 0.94-1.71, 50.2-90m, 40-70mm and 71-80% respectively. Because of their parabolic shape, they can focus the sun at 30-60times its normal intensity on a receiver pipe located along the focal line of the trough. Synthetic oil circulates through the pipe and captures this heat reaching temperatures of 390^0C.The hot oil is pumped to a generating station and routed through a heat exchanger to produce steam. Finally, electricity is produced in a conventional steam turbine.

2.5 Potential PTC application on biomass driers

There are several established methods, plus some promising technology, for dying biomass fuels for use in combustion boilers and gasifiers. Drying biomass provides significant benefits to boiler operation, but they must be balanced against increased capital and operating costs. These driers derive the heat from fossil fuels, steam flue gases and electricity whose costs are high and impact negatively on the

environment. This has prompted the need to adopt renewable energy sources for generating the heat required for drying. A parabolic trough concentrator capable of generating hot air above 100^0C can be adopted.

A general description of the most common types of dryers for biomass drying, the associated capital costs, heat requirements and comments on safety and environmental issues is presented below.

2.5.1 Flash Dryers

In these dryers, the solids are mixed with a high-velocity hot air stream. There is intimate contact of the solids with the air resulting in very rapid drying. A single operation provides mixing, heat transfer and mass transfer to dry a solid. The solids and air are separated using a cyclone, and the gases continue through a scrubber to remove any entrained particulate material [**7**].

Because of the short drying time in a flash dryer, the equipment is relatively more compact. However, the electricity consumption is higher because of the faster air flows through the unit and because biomass must pass through a shredder or grinder to reduce its size so it can be suspended in the air stream. [**6**]

To reduce the high costs incurred in the electricity consumed to heat the air, a PTC can be incorporated to generate the hot air.

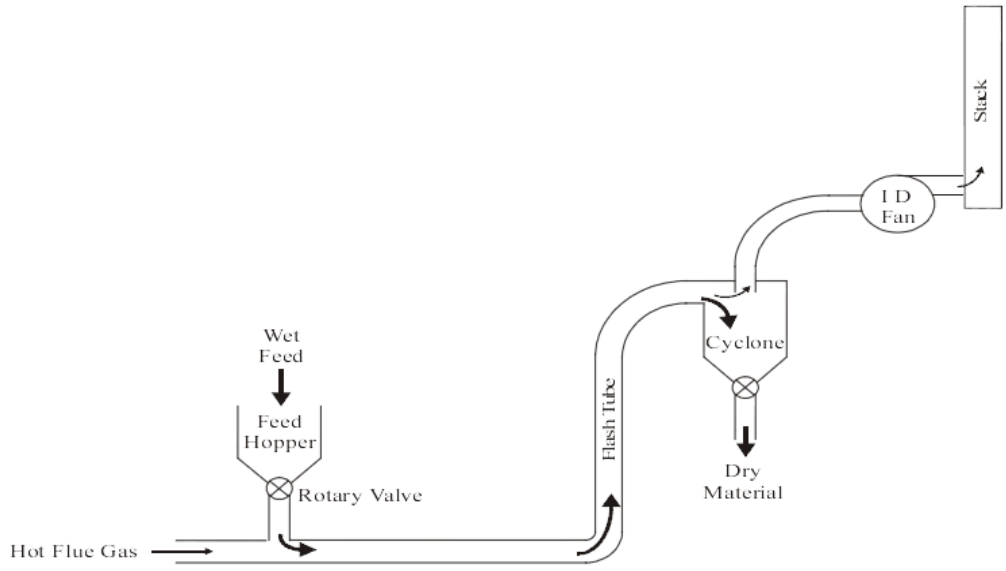

Figure 2.12: Flash dryer [**7**]

2.5.2 Rotary dryers

It consists of a horizontally inclined rotating cylinder. Material is fed at one end and discharged at the other end. In direct-type rotary dryers, hot gases move through the cylinder in direct contact with the material, either with or against the direction of its flow. The cylinder is equipped with flights, which lift the material and shower it down through the hot gas stream.

This dryer is formed by rotary body, lifting blade, driving device, supporting device and sealing ring. The dryer has advantages of reasonable structure, high efficiency, low energy consumption and convenient for transportation.

If contamination is not a concern, hot flue gas can be fed directly into the dryer. Other options include using a burner or steam heater to raise the temperature of incoming air. A PTC can also be utilized at this point to generate the hot air for the drying purposes. This way, integration of solar into the drying process of of biomass would be achieved.

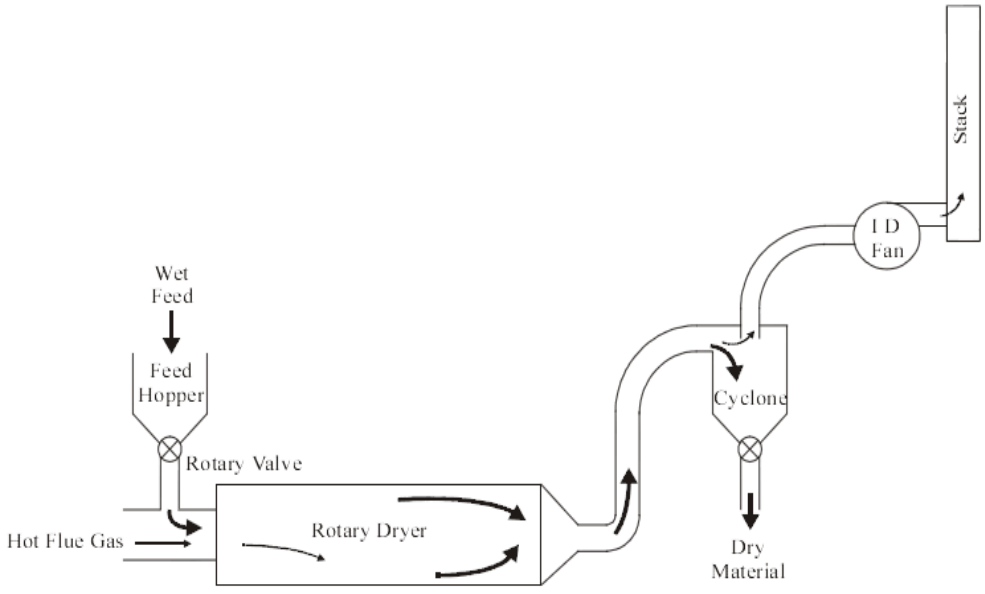

Figure 2.13: Rotary dryer [**7**]

2.5.3 Disk dryers

For smaller flows of material, a disk dryer is an option. In a disk dryer, solids are heated by condensing steam inside of a central shaft with many hollow disks that increase the area for heat transfer. Fingers mix the material and act to keep the heat transfer surfaces free of build up.

The disk dryer can be operated under a vacuum or under pressure, and the condensate from inside the heating shaft can be recovered and returned to the boiler.

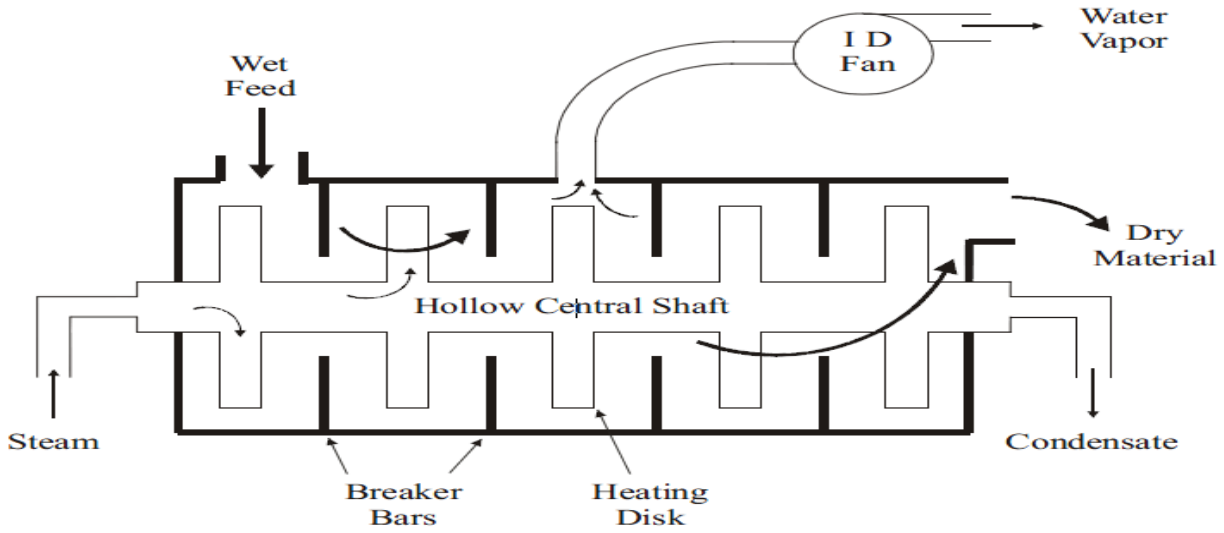

Figure 2.15: Disk dryer

2.5.4 Cascade dryers

Cascade dryers are commonly used for grain drying but they can be used for other types of biomass. Material is introduced to a hot stream of air as it enters an enclosed chamber. The material is thrown into the air, then falls, or cascades, back to the bottom to be lifted again. Some of the material is drawn out through openings in the side of the chamber that control the residence time and amount of drying. The typical drying time for a cascade dryer is a couple of minutes (MacCallum et al. 1981).

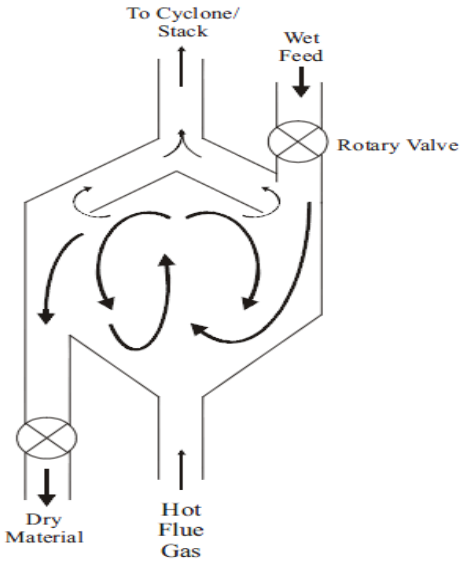

Figure 2.14: Cascade dryer [7]

CHAPTER 3

METHODOLOGY

3.0 Introduction

In this chapter, the methodology is presented. It begins with the design, then fabrication of the orifice plate, experimentation, data collection and finally analysis of data.

3.1 THE DESIGN OF AN ORIFICE METER

3.1.1 Introduction:

An orifice meter is used to measure the mass flow rate of air. It mainly consists of an orifice plate which is a thin flat plate with a hole in the middle. The orifice plate restricts the flow and develops a differential pressure which is proportional to the square of mass flow rate.

All the parameters were determined in line with BS EN ISO 5167-2:2003 (Orifice Plates).

3.1.2 Orifice Plate

The orifice plate shall be circular and concentric with the pipe centerline. The faces of the plate shall be flat and parallel to each other [**15**].

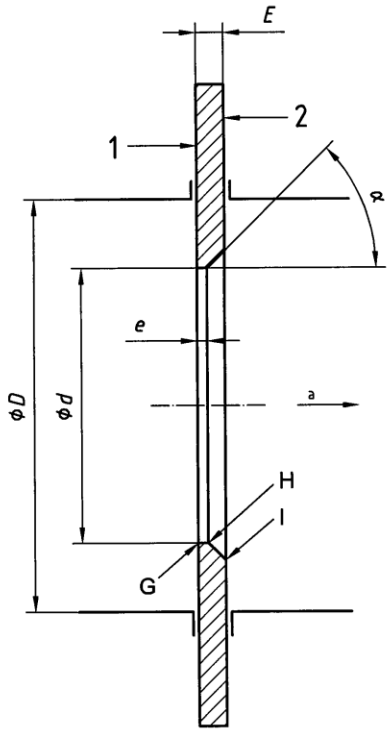

Figure 3.1: Standard orifice plate [**15**].

Key:

1-upstream face
2-downstream face
a- direction of flow
e- thickness of the cylindrical part of the orifice
E-thickness of the orifice plate
α-angle of bevel
G-upstream edge
H, I-downstream edges
D-pipe diameter
d- orifice diameter

3.1.2.1 Parameters

3.1.2.1.1 Thickness of the cylindrical part of the orifice, e
The thickness shall fall within the range $0.005D \leq e \leq 0.02D$

Taking the upper limit of 0.02D;

$$e=0.02\times50.8=1.06\approx1mm$$

3.1.2.1.2 Thickness of the orifice plate, E
The thickness shall fall within the range $e \leq E \leq 0.05D$
And also for $50mm \leq D \leq 64mm$, E of up to 3.2mm is acceptable.
Since our D falls within the range, we shall use E=3.2mm

Hence the beveled part shall have a thickness of (E-e)

$$E-e=3.2-1=2.2mm$$

3.1.2.1.3 Angle of bevel, ά
This angle shall fall within $30° \leq \alpha \leq 60°$
An angle of $\alpha=45°$ was selected.

3.1.2.1.4 Diameter of orifice, d
The diameter of the orifice shall be determined by the beta ratio, β, which is defined as;

$$\beta_1=d/D$$

β_1 shall fall within $0.10 \leq \beta_1 \leq 0.75$
We shall adopt a beta ratio, $\beta_1=0.5$
Hence our $d=0.5\times50.8=25.4mm$

3.1.3 Upstream and downstream pipes

The upstream and downstream lengths are determined for $\beta_1 = 0.5$ considering concentric expanders (see appendix)

For zero additional uncertainities,

The upstream length:

$$20D = 20 \times 50.8 = 1016mm$$

The downstream length:

$$6D = 6 \times 50.8 = 304.8mm$$

3.1.4 Pressure tappings

D and D/2 tappings shall be used.

Where both D and D/2 are measured from the upstream face of the orifice plate.

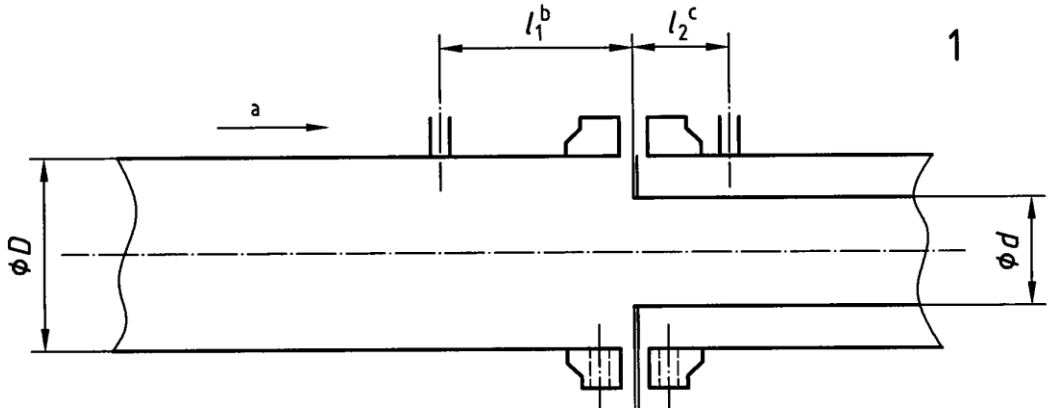

Figure 3.2: D and D/2 pressure tappings [**15**].

In this case **l_1^b=D=50.8mm**

l_2^c=D/2=25.4mm

For orifice plate with D and D/2 tappings:

d≥12.5mm

50mm≤D≤1000mm

0.1≤ β_1≤0.75

Actual design drawings are provided in the appendix.

3.2 Fabrication of Orifice Meter

The orifice meter consists of three major components. These are the orifice plate, upstream and downstream lengths, and the pressure tappings. All drawings of this orifice meter were prepared.

3.2.1 Sizing of the orifice meter

3.2.1.1 The orifice plate

A 3.4mm thick irregular piece of sheet metal was obtained from the Mechanical Engineering Workshop. An 88mm diameter piece was cut from the sheet metal using a lathe machine. Facing was done on both sides of the circular plate reducing the thickness to 3.2mm. A drill bit of was then used to drill a hole at the centre of the plate. A bevel section of thickness 2mm at an angle of 45° was then cut. A reamer was used to enlarge the hole to a diameter of 25.4mm.

Figure 3.3: Orifice plate

3.2.1.2 Downstream and upstream pipes

The orifice plate was to be fitted into a 50.8mm diameter pipe. A cutting disc was mounted onto a grinder and used to cut the pipe into 1016mm and 304.8mm for the upstream and downstream lengths respectively. The cut faces were ground and filed to near flatness. On the upstream pipe, a 7.3 mm hole was drilled at distance 50.8mm from the cut face. This hole was used to fit the upstream pressure tapping. Another 7.3mm hole was drilled on the downstream pipe at a distance of 22.2mm from the cut face.

A 3mm thick piece of sheet metal was used to make two flanges. Two 88mm diameter pieces were cut from the sheet metal using a lathe machine. A cutting tool was used to cut off a 50.8mm diameter piece from each flange. A momentum press machine was then used to flatten the flanges.

3.2.1.3 Pressure tappings

A 144.2mm copper rod was obtained from the workshop. It had an outside diameter of 7.3mm and an inside diameter of 3.0mm. The rod was then flattened using the momentum press. A hack saw was used to cut it into two equal pieces of length 72.1mm. One end of each piece was filed to obtain a bevel shape for easy fitting into the holes drilled into the upstream and downstream pipes.

3.2.1.4 Gaskets

Two 88mm diameter rubber gaskets were cut using a blade. Each gasket was then placed onto a welded flange and a circular piece was cut off using a hammer.

Figure 3.4: A gasket

3.2.2 Assembly of the orifice meter

3.2.2.1 Drilling of fastening holes

A hole of 6.5mm diameter was drilled on both flanges and the orifice plate along the circumference of the pitch circle. A metal rod was used to align the three holes. The three pieces were then welded together by spot welding along their circumferences. Three other similar holes were then drilled at equal distances from each other along the pitch circle circumference using a drilling machine.

3.2.2.2 Welding of the flanges

One flange and the cut face of the upstream pipe were placed onto the floor and a square was used to ensure squareness between the flange and the surface of the pipe. The flange was then joined to the pipe by welding.

The procedure above was repeated using the downstream pipe.

3.2.2.3 Brazing of the pressure tappings

One pressure tapping was inserted in the hole drilled on the upstream pipe. A square was used to ensure that it was perpendicular to the surface of the pipe. The tapping was then joined to the pipe by brazing. The procedure above was repeated using the downstream pipe.

Figure 3.5: Downstream length complete with pressure tapping

3.2.2.4 Joining the orifice plate to the flanges

The orifice plate was joined to the flanges in between two gaskets using four nuts and bolts. (See figure 3.6)

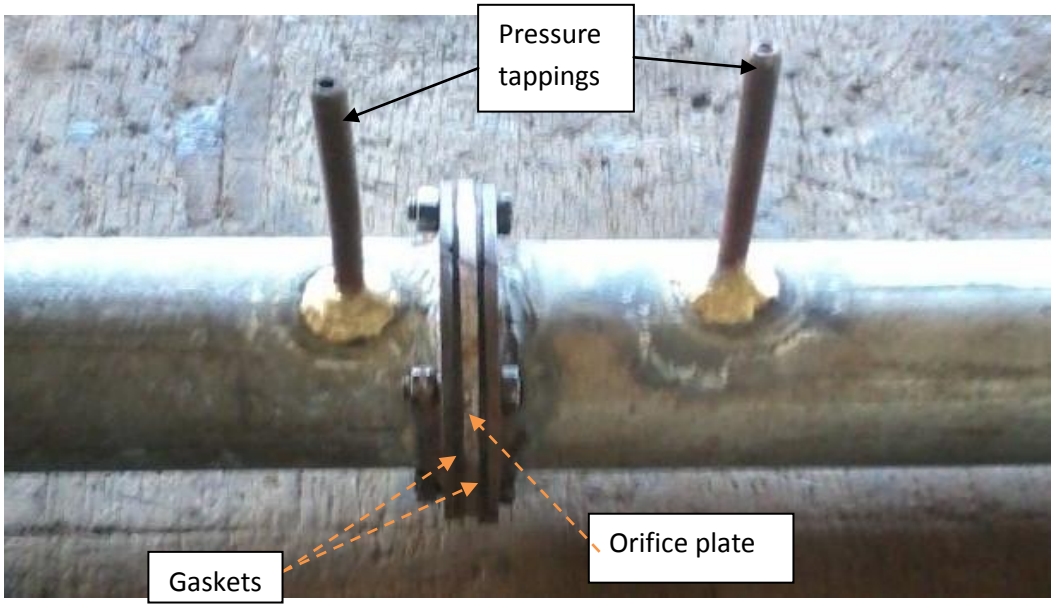

Figure 3.6: Fully assembled orifice meter

3.3 Performance testing of the PTC

3.3.1 Experimental procedures

The parabolic trough concentrator was set for performance evaluation test at the University of Nairobi. The experiment was set up as shown in **figure 4.4** .

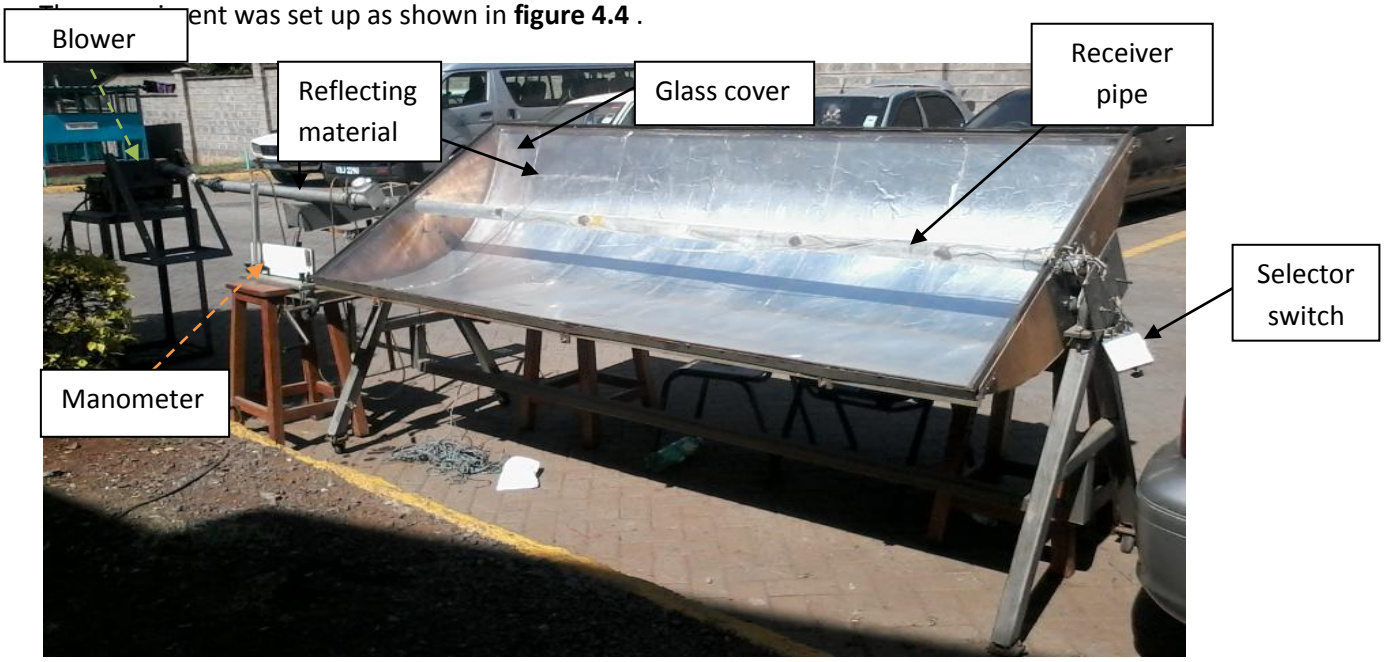

Figure 3.7: Experimental set up

The parabolic trough collector is manually tracked on each day before the reading starts so that the solar radiations fall perpendicular to the plane of aperture area. When the solar radiations fall on the aperture area of the parabolic trough collector, they are concentrated on the absorber tube. This causes the heat transfer from the surface of the absorber tube to the air flowing inside the absorber tube and air gets heated up.

The parameters recorded during the test were: ambient temperature T_{amb}, air inlet temperature T_{in}, outlet temperature $T_{o,}$ surface temperatures, irradiance, and pressure difference Δh. The experiments were carried out between 1000Hrs and 1600Hrs on selected days. During the experiments the PTC was placed in an area free from shadows and the mass flow rate, set. The aperture plane was aligned perpendicular to the sun using the manual tracking system. This was achieved by ensuring that the reflection of the sun's rays covered the lower half of the receiver pipe.

3.3.2 Data collection

The objective of the experiments was to heat air using a PTC at different mass flow rates to a temperature of 100°C-110°C. The data collected was used to evaluate the performance.

3.3.2.1 Temperatures

The air inlet, outlet and ambient temperatures were measured and recorded at intervals of 2 minutes for various mass flow rates on selected days. A dry bulb thermometer was used to measure the ambient temperature. A probe connected to a digital thermometer was inserted at the downstream end of the orifice meter at a point just before the concentrator and aided in measuring the inlet temperature. Thermocouple wires, type J were connected to a digital thermometer and aided in the determination of the outlet and receiver pipe surface temperatures.

3.3.2.2 Flow rate

A constant mass flow rate was used throughout a selected day. A manometer connected to an orifice meter was used to measure the pressure difference across the orifice plate. This differential pressure was then used to calculate the mass flow rate. A variant was used to set the mass flow rate on each day.

3.3.2.3 Solar radiation

A Henni solarimeter was used to measure total solar radiation intensity at intervals of 2 minutes. The solarimeter sensor was attached on a bracket bolted on the side of the trough as shown in the **figure 3.5**.

Figure 3.5: Solarimeter sensor

3.4 PTC specifications

Reflector material used was aluminium foil.

A 50.8mm diameter galvanized iron pipe was used as the receiver tube.

TABLE 3.1: PTC specifications [16]

Specification	**Value**
Length **(L)**	*2.4m*
Aperture**(W)**	*1.03m*
Aperture area**(A_p)**	*2.472m^2*
Rim angle**(θ_r)**	90^0
Reflectivity of reflector(ρ)	*0.88*
Receiver absorptivity(α)	*0.65*
Receiver emissivity(ε)	*0.28*
Stefan Boltzmann constant(σ)	$5.67 \times 10^{-8} W/m^2K^4$
Glass cover transmittance(τ)	*0.85*
Concentration ratio(C)	6.1356

3.5 Heat transfer relations

The following dimensionless numbers will be useful for analysis.

$$Nu = \frac{hD}{k} \; ; \quad Re = \frac{UD}{\upsilon} ; \; Pr = \frac{\mu C_p}{k} ; \; St = \frac{h}{\rho C_p}$$

I. Forced convection through a duct

In the PTC, forced convection occurs through the pipe since air is blown through it by the fan. [**8**]

$$Nu_D = 3.66 + \frac{0.0668(D/L)Re.Pr}{1+0.04[(D/L)Re.Pr]^{2/3}} \; valid \; for \; 0.5 < Pr < 100 \; and \; Re < 2100. \quad \text{.....3.1}$$

$$Nu_D = \frac{\frac{f}{8}\times(Re-1000)\times Pr}{1+12.7\sqrt{\frac{f}{8}\times\left[Pr^{\frac{2}{3}}-1\right]}} \; valid \; for \; 0.5 \leq Pr \leq 2000 \text{and } 3000 \leq \text{Re} \leq 5 \times 10^6 \quad \text{.....3.2}$$

II. Natural convection

The following general correlation suggested by Churchill and Chu would be useful over a wide range of GrPr. [**9**]

$$Nu_D = \left(0.6 + \frac{0.387R(Gr.Pr)^{\frac{1}{6}}}{\left[1+\left(\frac{0.559}{Pr}\right)^{\frac{9}{16}}\right]^{\frac{8}{27}}} \right)^2 \quad for\ 10^{-5} \leq Gr.Pr \leq 10^{12}$$ 3.3

$$Ra = GrPr = \frac{g\beta\,(T_s - T_a)L^3}{\upsilon}\Pr \quad for\ 10^{-6} \leq Ra \leq 10^{12}$$ .....3.4 [7]

The air properties are determined at mean film temperature.

Natural convection is depicted by the action of wind which carries away masses of air as it flows past the setup. This majorly gives rise to heat losses. Natural convection heat transfer coefficient is obtained by the expression below: [**10**]

$$h_{wind} = \frac{k_{air}}{D_o} Nu_D \qquad \text{For } \left({Gr}/{Re^2}\right) \geq 1$$ 3.5

3.5.1 Transmittance - absorptance product

It refers to the ratio of flux absorbed in the receiver to the one incident on cover system. The transmittance of the glass cover was 0.85 and the absorptivity of galvanized iron was 0.65.The product of transmittance-absorptance was determined to be:

$$\tau\alpha = 0.85 \times 0.65 = 0.5525.$$

Collector heat removal factor FR is calculated from[**11**]:

$$F_R = \frac{\dot{m}C_p}{A_o U_l}\left(1 - e^{\frac{-A_o F' U_l}{\dot{m}C_p}}\right)$$.....3.6

Collector efficiency factor F' was also obtained from equation [**11**]:

$$F' = \frac{{1}/{U_l}}{\frac{1}{U_l} + \frac{D_o}{h_f D_i} + \left(\frac{D_o}{2k} ln \frac{D_o}{D_i}\right)}$$ 3.7

Collector flow factor, F'' is calculated from:

$$F'' = \frac{F_R}{F'}$$.....3.8

Actual useful energy obtained from parabolic trough concentrator is given as:

$$Q_u = \dot{m}C_p(T_o - T_i)$$.....3.9

3.5.2 Heat losses analysis

Solar radiation is mainly absorbed at the outer surface of the absorber tube as heat. Part of the absorbed heat is transferred to the working fluid by conduction through tube wall and by convection from inner surface of the tube to the fluid. Part of the heat is lost by radiation to the inner surface of the glass cover and then by conduction from the inner surface of the glass to the outer surface of the glass. The heat is dissipated to ambient from the outer surface of the glass by two mechanisms:

a) Convection to the surrounding air $[\mathbf{12}]$:

$$h_{conv} = 0.0191 + 0.006608U_{wind} \quad \text{.....3.11}$$

b) Radiation to the surrounding surfaces(buildings and sky) $[\mathbf{13}]$:

$$h_{rad} = \epsilon\sigma(T_s + T_a)(T_s^2 + T_a^2) \quad \text{.....3.12}$$

Overall heat loss coefficient is obtained from $[\mathbf{13}]$:

$$U_l = h_{conv} + h_{rad} \quad \text{.....3.13}$$

The total heat lost will therefore be$[\mathbf{10}]$:

$$Q_{loss} = U_l A_o (T_s - T_a) \quad \text{.....3.14}$$

3.5.3 PTC Efficiency.

The efficiencies determined included:

1. Optical efficiency

This is the fraction of light power transmitted from the aperture of a concentrator to the receiver surface. It depends on the optical properties of the PTC materials, collector geometry and imperfections in reflector. The expression for optical efficiency is$[\mathbf{14}]$:

$\eta_o = \rho\alpha\tau$.....3.15

2. Theoretical thermal efficiency $[\mathbf{10}]$

$\eta_{th} = \frac{Q_{th}}{IA_{ap}}$.....3.16

3. Overall thermal efficiency $[\mathbf{10}]$

$$\eta_{overall} = \frac{Q_{actual}}{IA_{ap}} = \eta_o (W - D_o)L \text{.....3.17}$$

3.5.4 Sample calculations for mass flow rate

Mass flow rates were calculated by using:

$$\dot{m} = CA_2\sqrt{2\rho_1(P_1 - P_2)}$$

For instance, mass flow rate on 26/02/14:

$\dot{m} = 0.62 \times \pi \times 0.0127^2\sqrt{2 \times 1.1515 \times (9810 \times 0.013)}$ =0.00538kg/s

An approximate value of 0.62 was adopted for C [**15**].

The mass flow rates used were as tabulated below:

Date	**Mass flow rate(kg/s)**
26/02/2014	0.00538
03/03/2014	0.008846
05/03/2014	0.00299
12/03/2014	0.004472
24/03/2014	0.006678
26/03/2014	0.007483
02/04/2014	0.001493

3.5.5 Sample calculations for useful energy

Useful energy is calculated using **equation 3.9**;

$Q_u = \dot{m}C_p(T_o - T_i)$

For instance on 26/02/2014 when a mass of 0.00538kg/s was used, $(\boldsymbol{T_o - T_i})$ at 0958hrs was 14.9^{o} C. Useful energy, $\boldsymbol{Q_u}$=0.00538$\times$ 1005.4×14.9=80.59J/s.

$\mathbf{C_p}$ was determined at mean bulk temperature. Other values are as plotted in graphs in the appendix.

CHAPTER 4

RESULTS AND DISCUSSIONS

4.0 Introduction

The experiments were carried out to investigate the performance of the PTC between 1000Hrs and 1600Hrs on selected days between 26th February and 02nd April 2014. Throughout the experimentation, the PTC was covered with a glass.

In order to have a numerical appreciation of the results, the PTC parameters given in **table 3.1** are utilized to determine the thermal behavior of the PTC.

Mass flow rates of between **0.001493Kg/s (0.1cmH_2O)** and **0.008846Kg/s (2.9cmH_2O)** were used to analyze the effect of mass flow rates on rise in temperature, useful energy and overall efficiency.

4.1 Outlet temperature

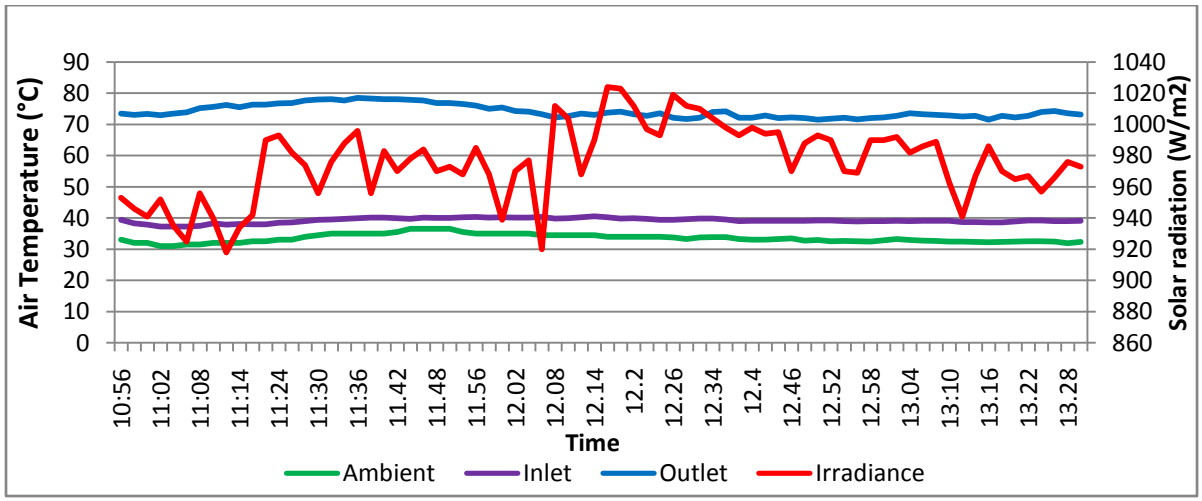

Figure 4.1: Variation of solar radiation, inlet and outlet temperatures with time taken on 03/03/14 at a mass flow rate of 0.008846Kg/s (2.9cmH_2O)

The highest outlet temperature recorded was 78.5°C at 1136hrs. The solar radiation here was 996W/m^2. The highest solar radiation was 1024W/m^2 at 1216hrs and the outlet temperature recorded was 73.8°C. The outlet temperature was expected to be highest at the highest solar insolation but this wasn't the case since there were numerous instances of cloud cover.

Figure 4.2: variation of solar radiation, inlet and outlet temperatures with time taken on 02/04/14 at a mass flow rate of 0.001493kg/s (0.1cmH_2O)

The solar radiation was fairly constant between 1044hrs and 1256hrs. It ranged from 863 W/m^2 to 965W/m^2. Within this range, the highest temperature was recorded and it was 105.6^{0}C at 1128hrs.This temperature was recorded when insolation was 903 W/m^2.

The highest temperature attained with the mass flow rate of 0.001493kg/s was higher than that obtained when using a mass flow rate of 0.008846kg/s. This is because less heat energy is required to heat air at a mass flow rate of 0.001493kg/s than 0.008846kg/s. The low mass flow rate indicates a low velocity of air through the pipe; this facilitates increased contact time of the air particles with the pipe hence the higher temperatures recorded.

Notably, at 1300hrs, 1404hrs and 1228hrs, there were instantaneous declines in the solar radiation to 182 W/m^2, 116 W/m^2 and 195 W/m^2 respectively. These are attributed to the sudden cloud covers. From the graph it is also evident that the effects of these declines on the outlet temperature were not immediate. This was attributed to the fact that the pipe took some time to cool due to its high heat capacity.

4.2 Efficiency

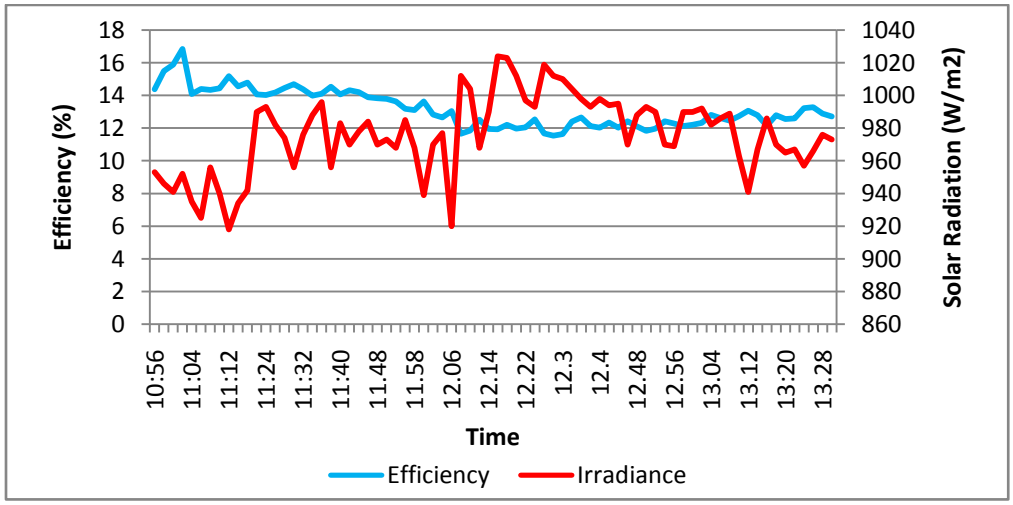

Figure 4.3: Variation of solar radiation and overall efficiency with time taken on 26/03/14 at a mass flow rate of 0.008846kg/s (2.9cmH_2O)

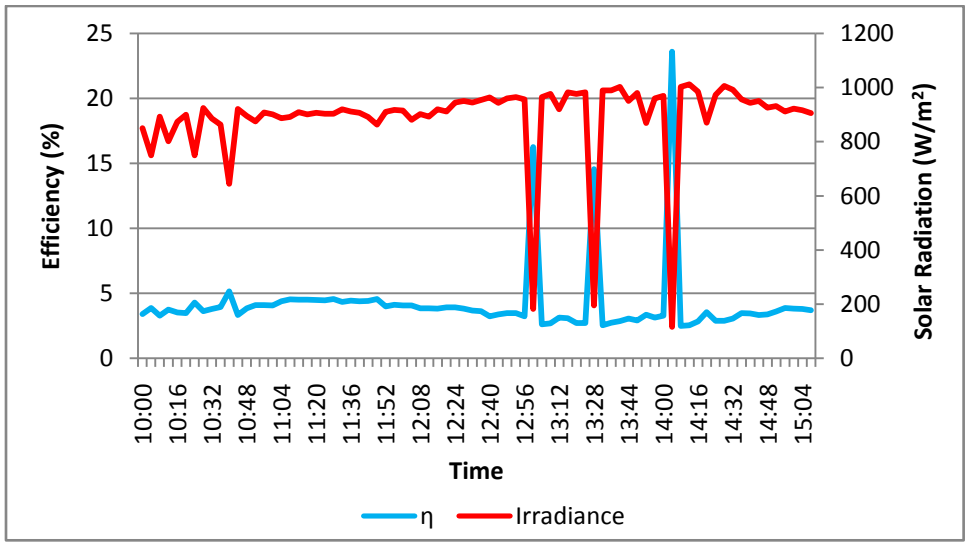

Figure 4.4: Variation of solar radiation and overall efficiency with time taken on 02/04/14 at a mass flow rate of 0.001493kg/s (0.1cmH_2O)

The overall efficiency of the PTC varied inversely with the solar radiation. From figure 4.4, an overall efficiency of 23.58% was calculated at 1404hrs. This was the highest overall efficiency at a mass flow rate of 0.001493kg/s and it occurred when the PTC was receiving the least radiation (116W/m^2).

An increase in insolation leads to high heat loss and therefore results into low overall efficiency **(see equation 3.17).**

4.3 Useful energy

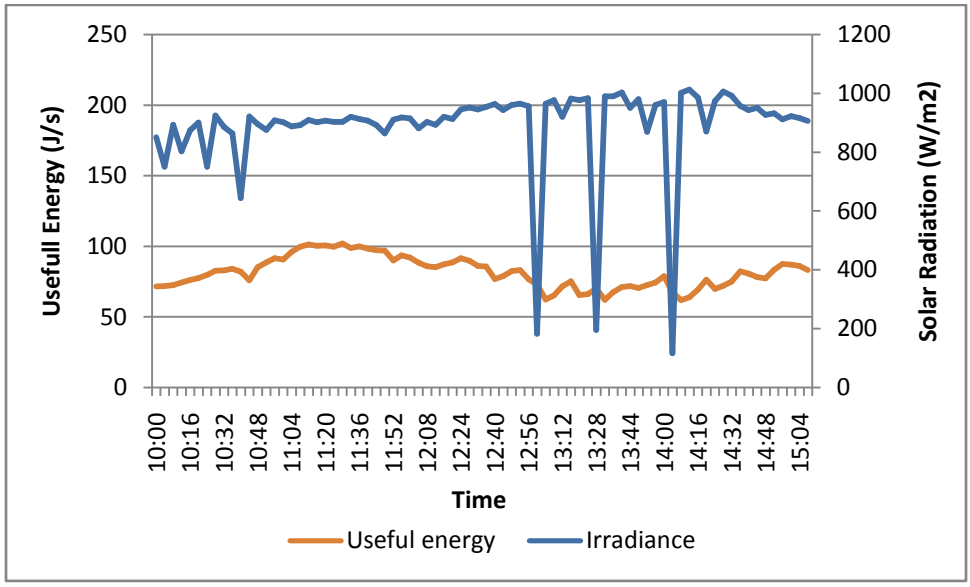

Figure 4.5: Variation of Useful Energy and Solar radiation with time taken on 02/04/14 at a mass flow rate of 0.001493kg/s (0.1cmH_2O)

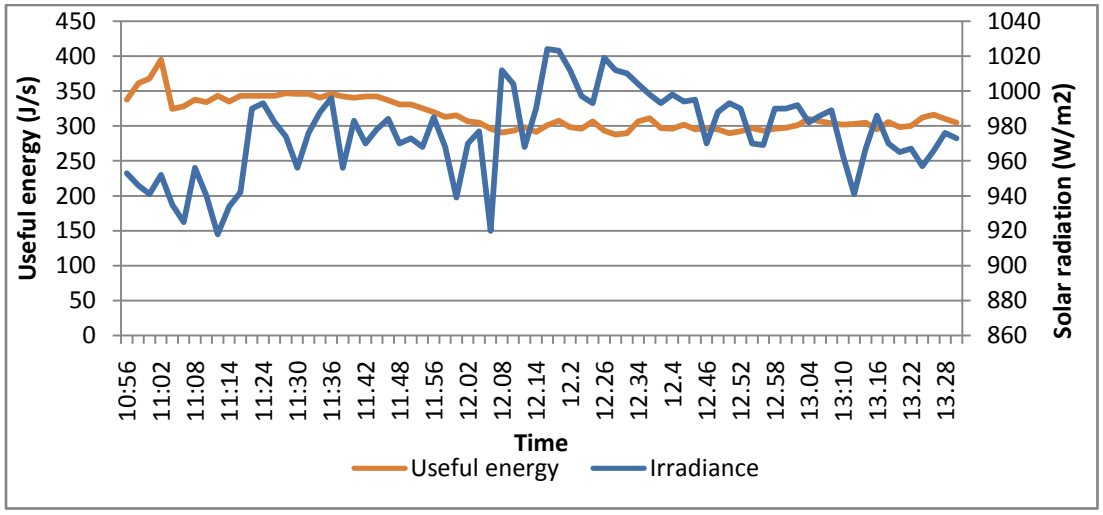

Figure 4.6: Variation of Useful Energy and Solar radiation with time taken on 26/03/14 at a mass flow rate of 0.008846kg/s (2.9cmH_2O)

From figures 4.5 and 4.6, it can be seen that useful energy increases with the solar radiation. However, the solar radiation and useful energy curves are out of phase. The useful energy curve lags the solar radiation curve. This is due to the fact that it takes some time for the change in solar radiation to be effected on the outlet temperature. The outlet temperature is a variable in the calculation of useful energy (see **equation 3.9**).

The highest useful energy obtained from the PTC with a mass flow rate of 0.001493kg/s was 101.86J/s at 1128hrs while that obtained with a mass flow rate of 0.008846kg/s was 395.05J/s at 1102hrs. The outlet

temperatures were 105.6°C & 72.9°C respectively. This is because whereas low flow rates have high temperature rises heat transfer coefficients are lower. Higher flow rates result to higher heat transfer coefficients and thus more actual useful energy is obtained.

4.4 Variation of Efficiency with mass flow rate.

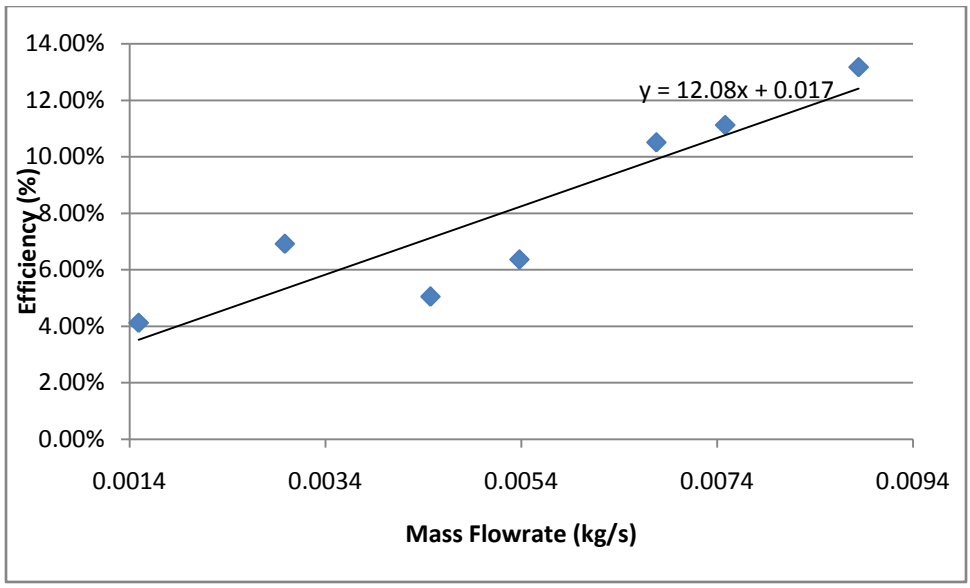

Figure 4.8: Variation of efficiency with mass flow rate.

The values of efficiency were average values calculated at times when solar radiation ranged between 950W/m^2 and 1000W/m^2 for various mass flow rates. From figure 4.8, it can be observed that efficiency increases with increase in mass flow rate (see **equation 3.17)**. Therefore efficiency is low at low mass flow rates. For example at a mass flow rate of 0.001493kg/s the efficiency was 3.5% and at a mass flow rate of 0.008846kg/s the efficiency was 10.74%.

CHAPTER 5

CONCLUSIONS AND RECOMMENDATIONS

5.1 Conclusion

The objectives of the study were to design and fabricate an orifice meter and to evaluate the performance of a PTC using different mass flow rates.

An orifice meter was successfully fabricated at the Mechanical Engineering Workshop, University of Nairobi. Its main components were an orifice plate, pressure tappings and upstream and downstream pipes. The orifice plate had an orifice diameter of 25.4mm and a thickness of 3.2mm. The upstream and downstream lengths were 1016mm and 304.8mm respectively. D and D/2 pressure tappings were employed. Calibration was however not done due to limited time.

The lowest and highest mass flow rates used during the study were 0.001493kg/s (0.1cmH_2O) and 0.008846kg/s (2.9cmH_2O) respectively. The highest temperature recorded while using a mass flow rate of 0.001493kg/s was 105.6°C while that recorded while using a mass flow rate of 0.008846kg/s was 72.9°C. It is therefore evident that higher outlet temperatures are obtained at low mass flow rates.

The maximum useful energy obtained from the PTC with a mass flow rate of 0.001493kg/s was 101.86J/s while that obtained with a mass flow rate of 0.008846kg/s was 395.05J/s. This indicates that useful energy is directly proportional to mass flow rate.

Average overall efficiencies calculated while using mass flow rates of 0.001493kg/s and 0.008846kg/s were 3.5% and 10.74% respectively. This implies that the efficiency increases with increase in mass flow rate.

5.2 Recommendations

An automatic tracking system should be incorporated to minimize tracking errors and hence improve the efficiency of the PTC.

Decreasing the width of the focal line would improve the concentration ratio and allow for a smaller receiver area which loses less radiation.

Radiation loss can be reduced via ε, as is done using selective coating on the radiation receiver, by limiting the area which radiates.

Concentration ratio could be improved by the use of a secondary concentrator, which further concentrates the already concentrated solar radiation coming from the parabolic trough reflector (funnel-shaped mirror system).

Materials with higher reflectivity than aluminium foil e.g aluminium sheet should be used since they can concentrate more rays of the sun hence increasing the efficiency of the PTC.

The receiver pipe should be painted black to increase its absorptivity. This would further increase the efficiency of the PTC.

REFERENCES

1. E. Zarza (2011) “Medium Temperature Solar Concentrators” , Solar Energy Conversion and Photoenergy systems, Vol. 1
2. KPLC Annual Accounts Report of financial year 2011/2012
3. Ekechukwu, O.V., Norton, B., 1999. Review of solar-energy drying systems II: An Overview of Solar Drying Technology. Energy Conversion & Management, Vol. 40, pp. 615-655
4. Werner Weiss, Josef Buchinger: Solar Drying- Establishment of a Production, Sales And Consulting Infrastructure for Solar Thermal Plants In Zimbabwe, Supported by the Austrian Development Cooperation.
5. A. Mokhtari, M. Yaghoubi, P. Kanan, A.vadiee.R. Hessami(2007) “Thermal and Optical Sudy of Parabolic Trough Collectors of Shiraz Solar Power Plant” Proceedings of The third International Conference on Thermal Engineering: Theory and Applications May 21-23,2007,Jordan
6. Jefferson L.G.C, Daniel R.G., Maria A.S., Silvia A.N., (2004) “Cyclone as a Sugarcane Dryer” , Chinese j. Chemical Engineering Vol.12 (6) pg 826-830.
7. Wade A. Amos “Report on Biomass Dying Technology”, Nov 1998, National Renewable Energy Laboratory
8. J. P. Holman, "Heat Transfer", McGraw-Hill, Fourth Edition, 1976.
9. Harlan H.Bengston, P.E (2010) “Convection Heat Transfer Estimation” SunCam online continuing education course
10. Duffie J.A, Beckman W.A (1980) “Solar Energy of thermal Processes” John Wiley & Sons, New York.
11. H. P. Gary and J. Prakash, "Solar Energy Fundamentals and Applications", New Delhi, www.Tata McGraw-Hill.Com, 2005.
12. Zhang L,Wang W, Yu Z, Fan L, Hu Y, Ni Y, Fan J, Cen K. An experimental investigation of a natural circulation heat tube system applied to a parabolic solar collector steam generation system. Solar Energy 2012; 86:911-919.
13. Yassen T.A (2012) “Experimental and Theoretical study of a parabolic trough solar collector” Anbar Journal for Engineering Sciences.
14. Hii, C.L; Law, C.L. (2012) “Solar drying of major commodity products. In solar drying: Fundamentals, Applications and Innovations, Ed.Hii, C.L, Ong, S.P, Jangam, S.V and Mujumdar”, A.S, ISBN-978-981-07—3336-0, published in Singapore, pg 73-94.
15. International Organization of Standards (ISO 5167-1:2003), Measurement of fluid flow by means of differential pressure devices, Part 2: Orifice plates.
16. W. Kariuki (2012) “Report on the Performance of a Parabolic Trough Concentrator Air Heater”, Master’s thesis.

APPENDIX

TABLE 1: DATA FOR MINIMUM MASS FLOW RATE

DATE:	02-04-14								
Man.:	0.1cmH2O		ṁ=0.001493kg/s						
Time	Irradiance	Ambient	inlet	Outlet	Time	Irradiance	Ambient	inlet	Outlet
10:00	850	25	33	80.2	12:36	954	30.5	39.5	96
10:04	750	25	33.6	81	12:40	963	30.5	39.3	90
10:08	893	25	33.8	81.6	12:44	943	31	39.8	91.8
10:12	802	25.5	34.2	83.3	12:48	960	31	39.8	94.3
10:16	874	25	34.4	84.7	12:52	965	31	40	94.9
10:20	900	25	35	86.1	12:56	956	31	39.7	90.3
10:24	750	25	35.2	87.8	13:00	182	29	38.4	86.5
10:28	924	26	35.5	90.1	13:04	965	31	38.9	80.1
10:32	885	26.5	35.7	90.5	13:08	977	31	39.9	82.9
10:36	863	26.5	35.8	91.3	13:12	920	31	39.7	87
10:40	644	25.5	36.2	90.4	13:16	982	31	39.9	89.5
10:44	921	26	36.4	86.5	13:20	976	31	39.6	82.8
10:48	895	26.5	36.7	92.9	13:24	983	31	39.8	83.5
10:52	875	27	36.6	95.1	13:28	195	29	38.1	84.3
10:56	908	27	36.8	97.3	13:32	989	29	37.9	78.9
11:00	901	27	37.1	97	13:36	990	30	37.8	82.3
11:04	887	28	37.4	100.9	13:40	1003	31	37.6	84.6
11:08	892	27	37.6	103.5	13:44	950	31	38.2	85.6
11:12	909	28	37.9	104.8	13:48	980	31	39.5	86
11:16	901	28	37.9	104.2	13:52	869	31	40.1	87.9
11:20	907	28	37.9	104.3	13:56	960	31	40.1	89.2
11:24	903	27.5	38	103.8	14:00	970	30.5	40.1	92.2
11:28	903	28	38.3	105.6	14:04	116	29.5	38.8	83.3
11:32	920	28	38.3	103.6	14:08	1002	31	39.9	80.8
11:36	912	29	38.4	104.4	14:12	1012	31	40.2	82.3
11:40	907	29	38.5	103.4	14:16	985	30.5	39.6	85.3
11:44	892	28.5	38.4	102.6	14:20	870	31	40.2	90.6
11:48	863	29	38.3	102.4	14:24	973	31	39.2	85.3
11:52	910	29	38.4	97.8	14:28	1006	31	39.7	87.2
11:56	918	29	38.7	100.5	14:32	992	31	40.6	90.1
12:00	915	29	38.6	99.4	14:36	957	31	40.7	95
12:04	881	29	38.9	97.3	14:40	943	31	40.6	93.8
12:08	902	29	38.5	95.2	14:44	950	31	40.7	92.3
12:12	893	29.5	38.8	95	14:48	926	31	40.4	91.4
12:16	920	29.5	38.9	96.5	14:52	932	30	39.9	94.9
12:20	912	30	39.5	98	14:56	911	30.1	39	96.7
12:24	945	29	39.1	99.5	15:00	922	30.5	39.2	96.7
12:28	951	29.5	39	98.2	15:04	916	30.5	39	95.8
12:32	945	29.5	39	95.8	15:08	906	30.5	38.6	93.5

TABLE 2: DATA FOR MAXIMUM MASS FLOW RATE

DATE:	03-03-14								
Man.:	2.9cmH2O		ṁ=0.008846kg/s						
Time	Irradiance	Ambient	Inlet	Outlet	Time	Irradiance	Ambient	Inlet	Outlet
10:56	953	33	39.4	77.1	12:16	1024	34	40.2	73.8
10:58	946	32	38.3	78.6	12:18	1023	34	39.8	74.1
11:00	941	32	37.9	79	12:20	1012	34	39.9	73.2
11:02	952	31	37.3	81.4	12:22	997	34	39.7	72.7
11:04	935	31	37.3	73.5	12:24	993	34	39.4	73.6
11:06	925	31.5	37.3	73.9	12:26	1019	33.7	39.4	72.1
11:08	956	31.5	37.5	75.2	12:28	1012	33.2	39.6	71.7
11:10	940	32	38.3	75.6	12:30	1010	33.8	39.8	72.1
11:12	918	32	37.9	76.2	12:34	1004	33.9	39.8	74
11:14	934	32	38.1	75.5	12:36	998	33.9	39.5	74.2
11:16	942	32.5	38	76.3	12:38	993	33.2	39	72.1
11:22	990	32.5	38	76.3	12:40	998	33	39.1	72.1
11:24	993	33	38.5	76.8	12:42	994	33	39.1	72.8
11:26	982	33	38.6	76.9	12:44	995	33.2	39.1	72
11:28	974	34	39	77.7	12:46	970	33.4	39.1	72.2
11:30	956	34.5	39.4	78	12:48	988	32.7	39.1	72
11:32	976	35	39.5	78.1	12:50	993	32.9	39.2	71.5
11:34	988	35	39.7	77.7	12:52	990	32.5	39.2	71.8
11:36	996	35	39.9	78.5	12:54	970	32.6	39	72.1
11:38	956	35	40.1	78.3	12:56	969	32.5	38.9	71.6
11:40	983	35	40.1	78.1	12:58	990	32.4	39	72
11:42	970	35.5	39.9	78.1	13:00	990	32.8	39	72.2
11:44	978	36.5	39.7	77.9	13:02	992	33.2	39.1	72.7
11:46	984	36.5	40.1	77.7	13:04	982	32.9	39	73.6
11:48	970	36.5	40	76.9	13:06	986	32.7	39.1	73.3
11:50	973	36.5	40	76.9	13:08	989	32.6	39.1	73
11:52	968	35.5	40.2	76.5	13:10	963	32.4	39.1	72.8
11:56	985	35	40.3	76	13:12	941	32.4	38.7	72.5
11:58	968	35	40.1	75	13:14	967	32.3	38.7	72.7
12:00	939	35	40.2	75.4	13:16	986	32.2	38.6	71.5
12:02	970	35	40.1	74.3	13:18	970	32.3	38.6	72.7
12:04	977	35	40.1	74.1	13:20	965	32.4	38.9	72.2
12:06	920	34.5	40.3	73.3	13:22	967	32.5	39.2	72.7
12:08	1012	34.5	39.8	72.2	13:24	957	32.5	39.2	74
12:10	1004	34.5	39.9	72.6	13:26	966	32.4	39	74.3
12:12	968	34.5	40.2	73.5	13:28	976	31.9	39	73.6
12:14	990	34.5	40.5	73	13:30	973	32.3	39.1	73.1

OUTLET TEMPERATURE, EFFICIENCY & USEFUL ENERGY GRAPHS

1.0 Manometer reading=0.4cm.H2O, ṁ=0.002986kg/s

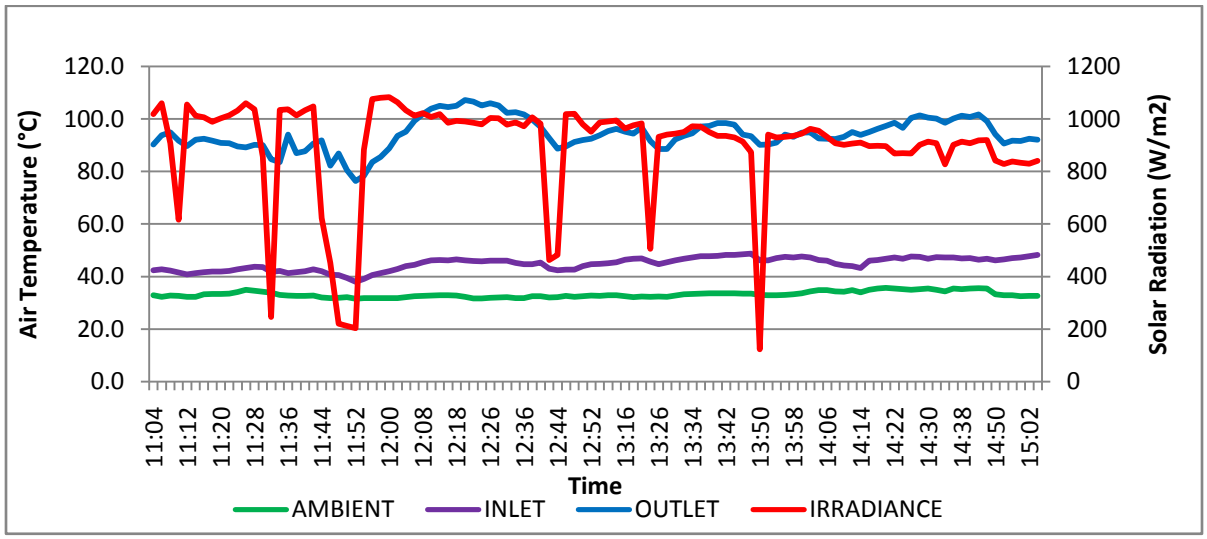

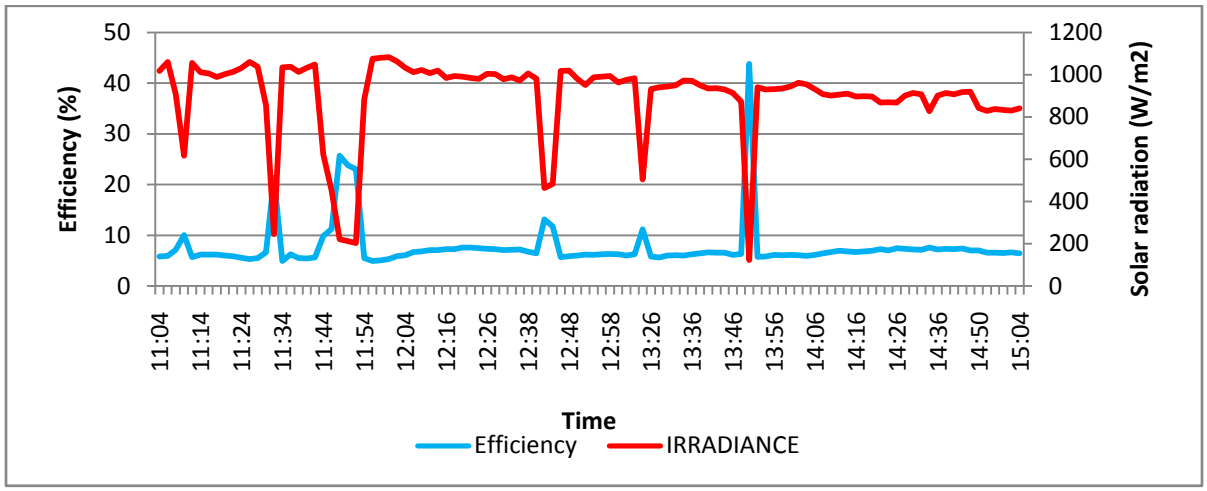

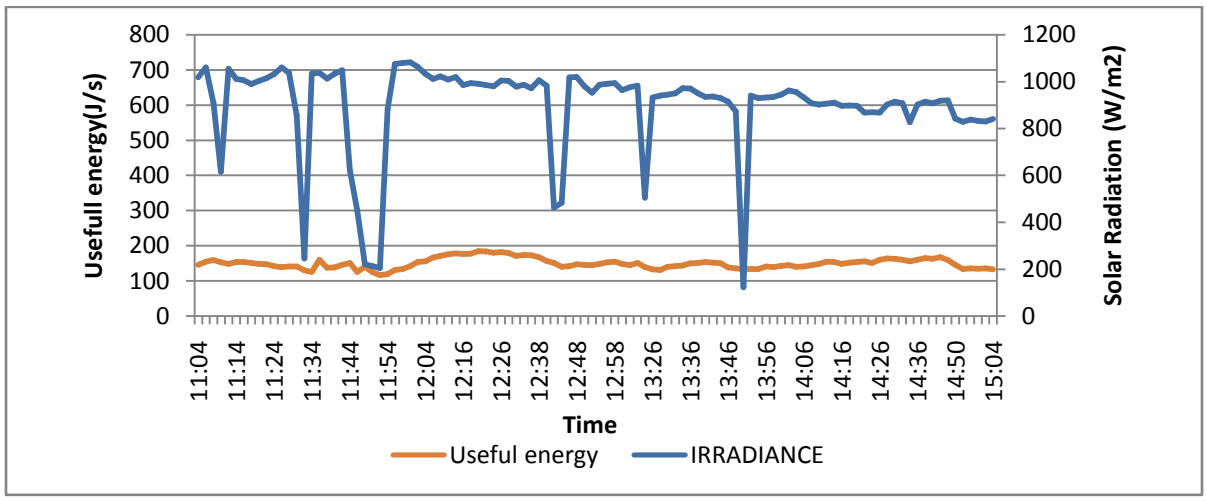

2.0 Manometer reading=0.9cm.H2O, ṁ=0.004472kg/s

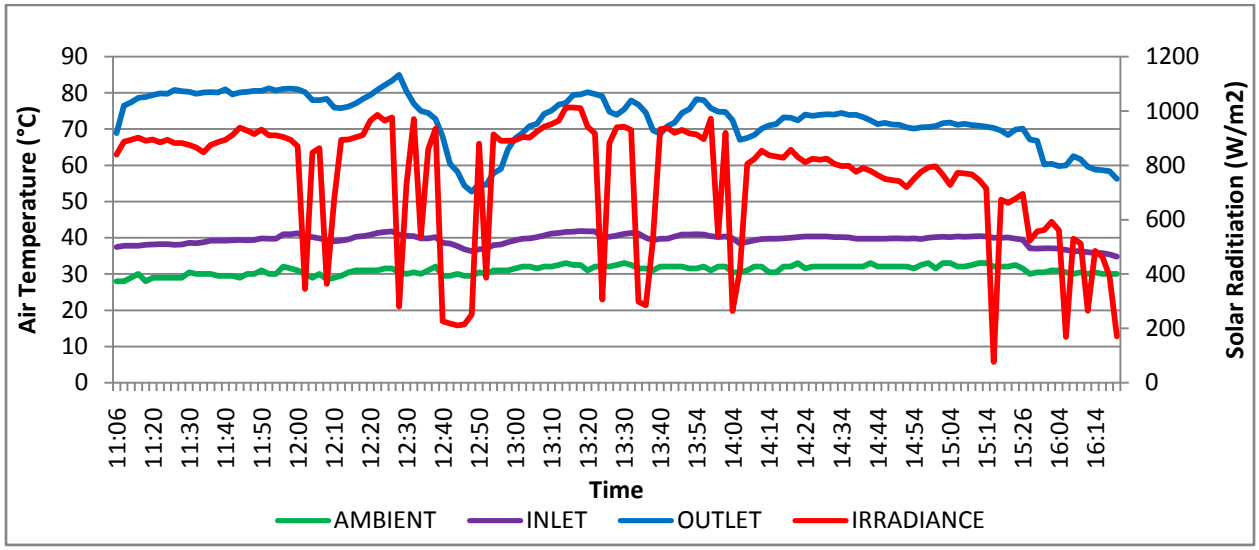

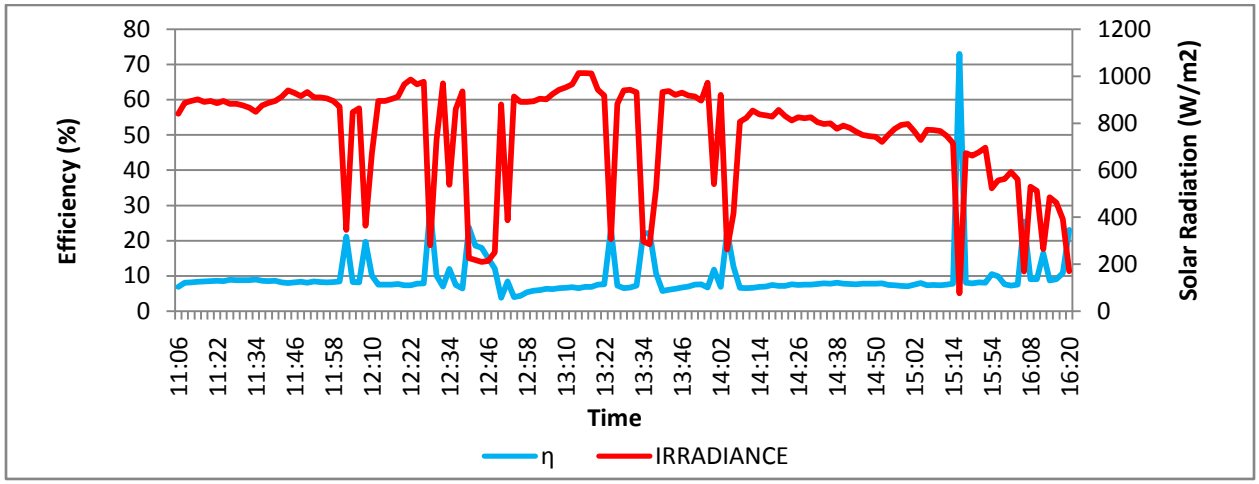

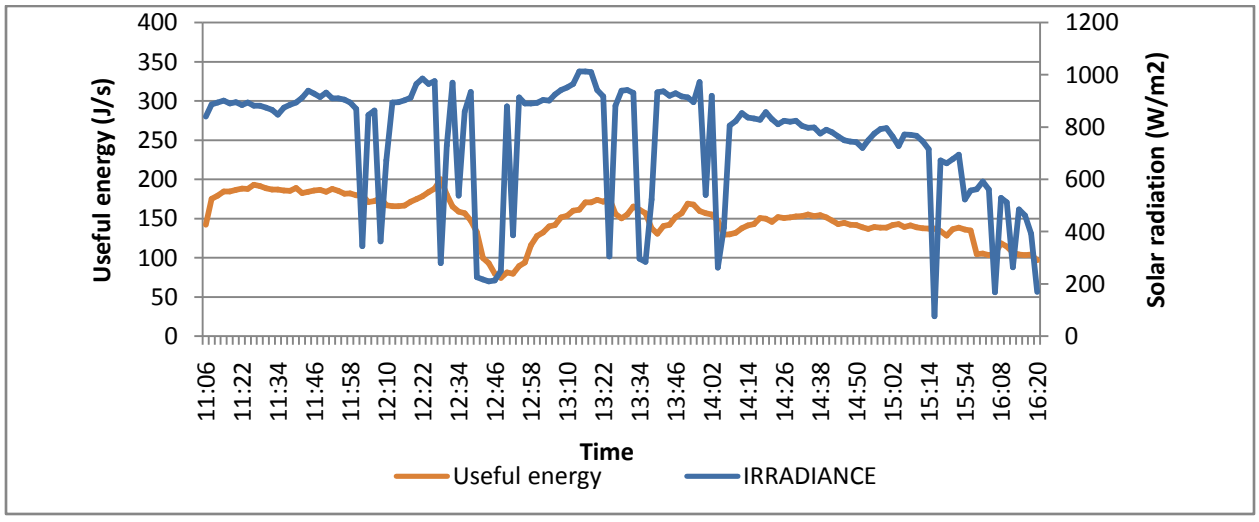

3.0 Manometer reading=1.3cm H2O, ṁ=0.00538kg/s

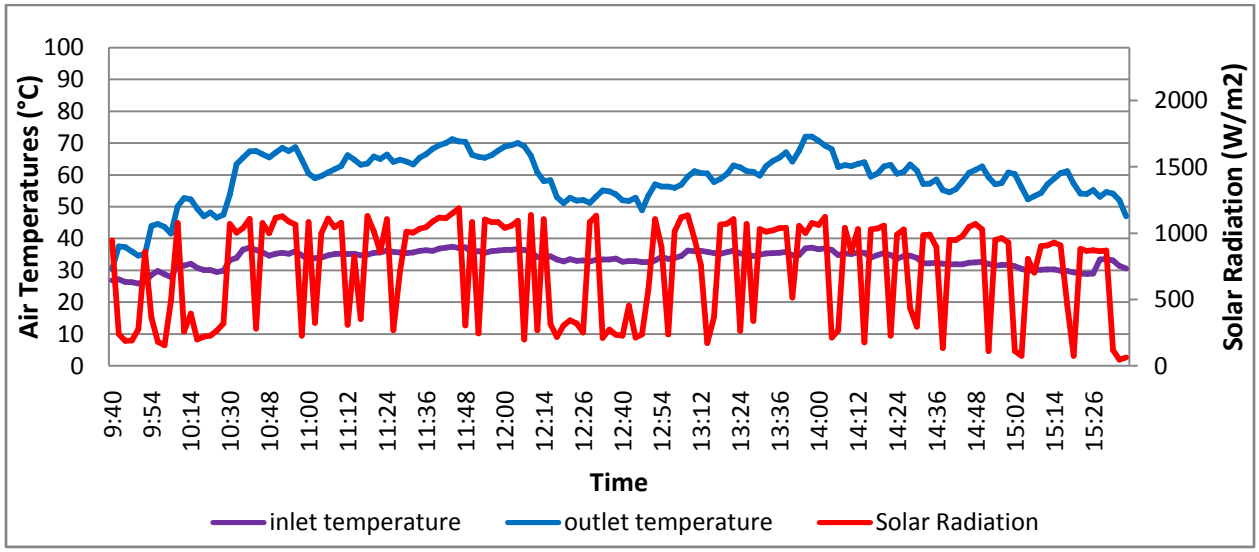

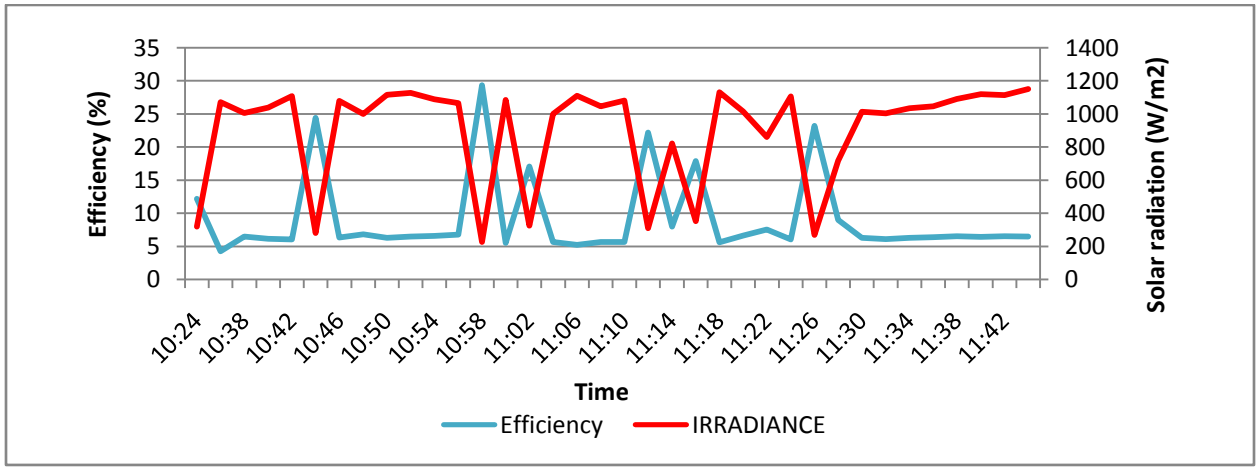

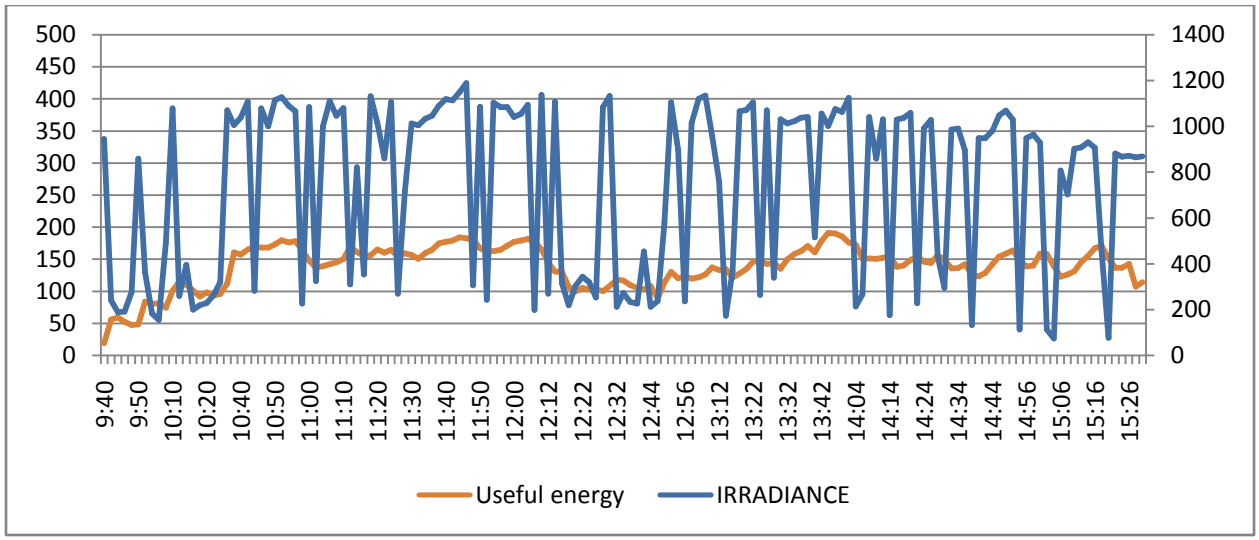

4.0 Manometer reading=2.0cm H2O, $\dot{m}$=0.00678kg/s

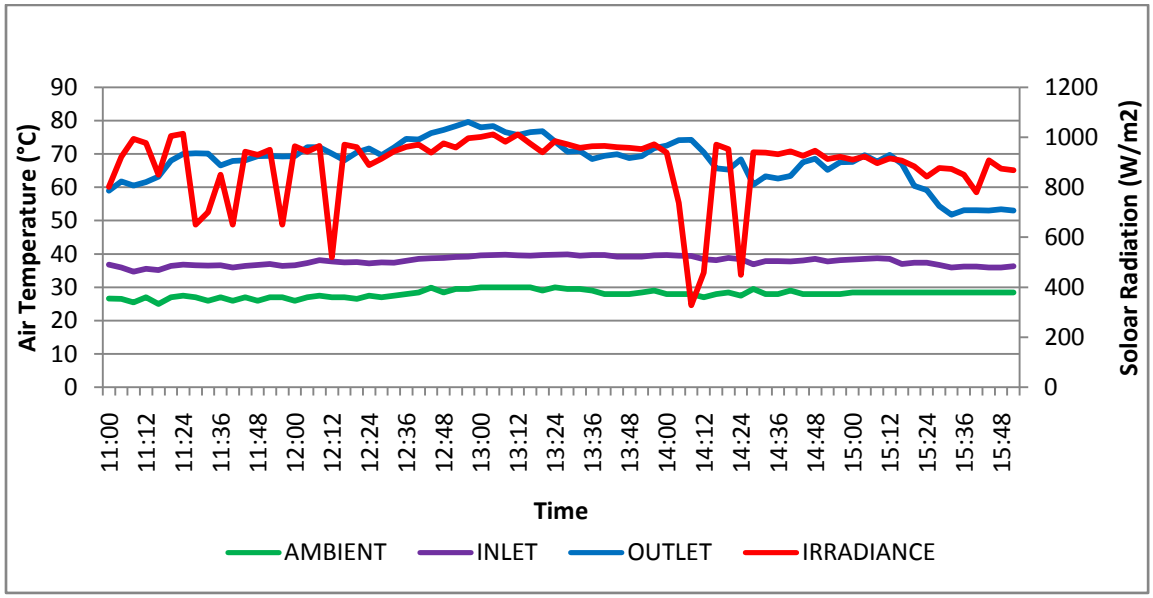

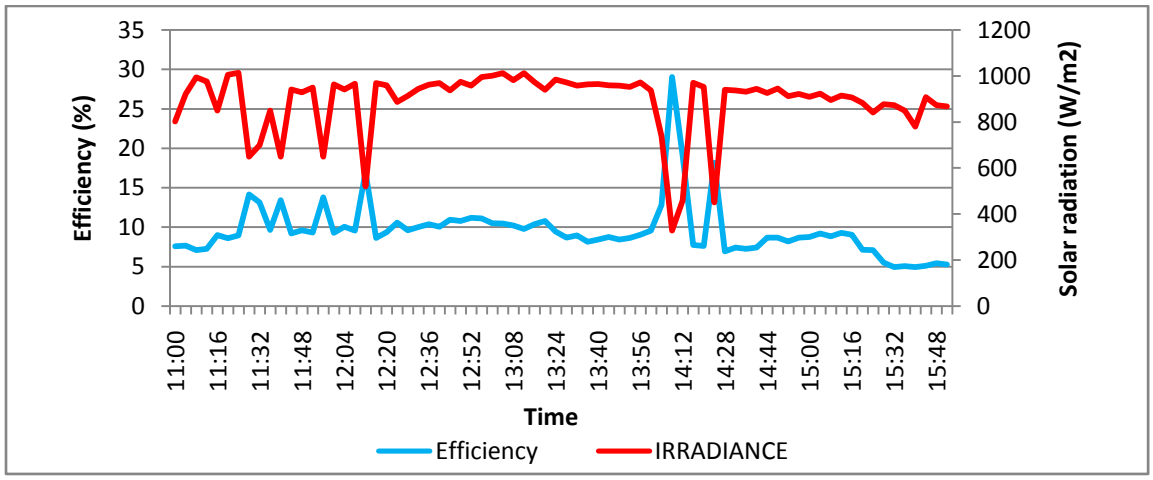

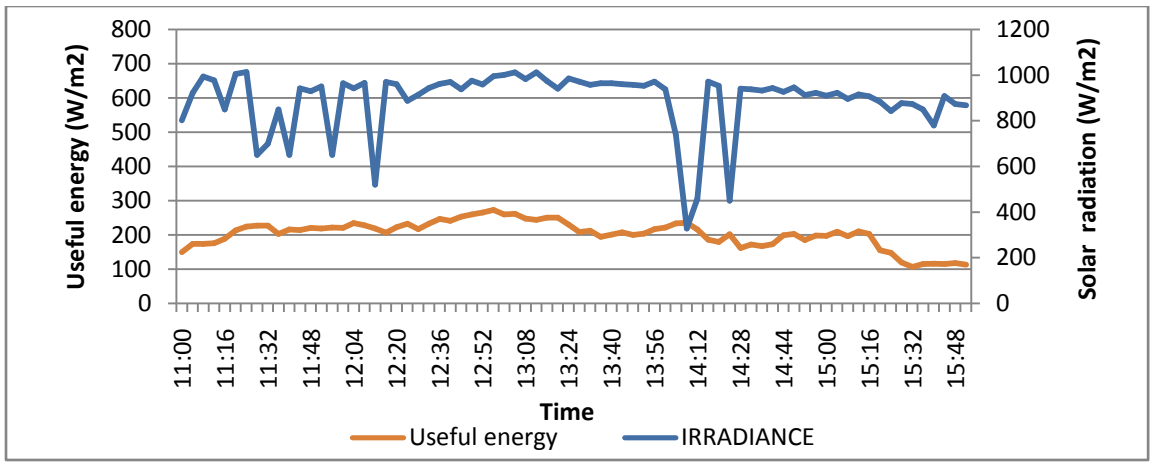

5.0 Manometer reading=2.5cm H2O, ṁ=0.007483kg/s